

PHOTOACCLIMATION in *Eutrema salsugineum*

A Thesis Submitted to the College of
Graduate Studies and Research
in Partial Fulfillment of the Requirements
for the Degree of Master of Science
in the Department of Plant Sciences
University of Saskatchewan
Saskatoon

By
Juan Lobo

PERMISSION TO USE

In presenting this thesis in partial fulfillment of the requirements for a postgraduate degree from the University of Saskatchewan, I agree that the libraries of this University may make it freely for inspection. I further agree that permission for copying of this thesis in any manner, in whole or in part, for scholarly purposes may be granted by the professor or professors who supervised my thesis work, or, in their absence, by the head of the Department or the Dean of the College in which my thesis work was done. It is understood that any copying or publication or use of this thesis or parts thereof for financial gain shall not be allowed without my written permission. It is also understood that due recognition shall be given to me and to the University of Saskatchewan in any scholarly use which may be made of any material in my thesis.

Requests for permission to copy or to make use of materials in this thesis in whole or in part should be addressed to:

Head of the Department of Plant Sciences
University of Saskatchewan
Saskatoon, Saskatchewan S7N 5A8
Canada

OR

Dean
College of Graduate Studies and Research
University of Saskatchewan
107 Administration Place
Saskatoon, Saskatchewan S7N 5A2
Canada

ABSTRACT

Eutrema salsugineum is an extremophilic model plant for stress tolerance studies. This study aimed to characterize the photoacclimation mechanisms of the Shandong and Yukon ecotypes of *Eutrema* under two growth irradiance regimes low- (LL) and high-light (HL). The experimental tools and techniques included physical measurements, pigment extractions and CO₂- and light-response curves to assess photoacclimation. The two ecotypes showed minor differences in the growth kinetics experiment across the light regimes utilized. Under LL the two ecotypes exhibited a similar performance in terms of growth with a slightly higher growth rate of the Yukon ecotype. When plants were grown under HL conditions growth was similar in both ecotypes for the first weeks, after that point the Shandong ecotype appears to grow at a faster rate compared to Yukon. The photosynthetic pigment analyses showed that the Shandong ecotype does not modify chlorophyll (Chl) *a:b* ratio as a photoacclimation mechanism in response to HL growth irradiance. This inability to modify pigment composition might make this ecotype prone to photoinhibition as observed in the results of this study. Conversely, the Yukon ecotype modifies its Chl *a:b* ratio in response to growth at a higher irradiance conferring this ecotype a higher tolerance to photoinhibition due to a photoacclimation of the light harvesting chlorophyll-proteins as a response to the increased growth irradiance. The gas exchange measurements showed a contrasting response of these two ecotypes. The Shandong ecotype exhibits higher rates of photosynthesis than Yukon when plants were grown under HL. It appears that Shandong is suppressing photorespiration as a photoacclimation mechanism to HL. The findings of this study confirm that these two ecotypes have different photoacclimation mechanisms to HL.

ACKNOWLEDGEMENTS

I would like to express my deepest gratitude to Dr. Gordon R. Gray for his encouragement, scientific guidance, patience and financial support during my studies.

I would also like to thank my graduate committee members: Dr. Yuguang Bai, Dr. Karen Tanino and Dr. Chris Todd for their time and advice in the completion of this thesis.

Special thanks to Dr. Ken Wilson for his always friendly advice and willingness to help with my project. Thanks to the staff of the Department of Plant Sciences especially Kendra and Marlene.

Also, I would like to thank my friends Cory Jacob, Jennara Field, Kirby Nilsen, Rishikesh Warale and Ian Willick for listening me and helping out during stressful times.

DEDICATION

This thesis is dedicated to my parents who always encouraged me to pursue my studies and supported me throughout the years. It is also dedicated to my beautiful wife Tatiana and adorable daughter Fabiana.

TABLE OF CONTENTS

PERMISSION TO USE	i
ABSTRACT	ii
ACKNOWLEDGEMENTS	iii
DEDICATION	iv
TABLE OF CONTENTS	v
LIST OF TABLES	viii
LIST OF FIGURES	ix
LIST OF ABBREVIATIONS	xi
1.0 INTRODUCTION	1
1.1 Hypothesis and Objectives	2
1.1.1 Hypothesis	2
1.1.2 Overall Objectives	2
1.1.3 Specific Objectives	2
2.0 LITERATURE REVIEW	4
2.1 Photosynthesis	4
2.1.1 Light Reactions	4
2.1.2 Carbon Reactions	7
2.2 Photorespiration	9
2.3 Photostasis.....	11
2.4 Photoacclimation	15
2.5 <i>Eutrema salsuginea</i>	17
3.0 MATERIALS AND METHODS	19
3.1 Plant Materials and Growth Conditions	19
3.2 Growth Analyses	19
3.2.1 Absolute Growth Parameters	19
3.2.2 Relative Growth Parameters	20

3.3 Photosynthetic Gas Exchange Measurements	20
3.3.1 Light Responses	22
3.3.1.1 Intrinsic Water Use Efficiency	22
3.3.2 CO ₂ Responses	22
3.3.3 Modelling	23
3.4 Pigment Determination	23
3.4.1 Chlorophyll and Carotenoids	23
3.4.2 Anthocyanins	24
3.5 Photoinhibition of Photosynthesis	24
3.5.1 Photoinhibition	24
3.5.2 Chlorophyll Fluorescence	25
3.6 Statistics and Experimental Design	25
4.0 RESULTS	26
4.1 Growth Analyses	26
4.1.1 Absolute Growth Parameters	26
4.1.2 Relative Growth Parameters	30
4.2 Pigments	39
4.2.1 Chlorophyll and Carotenoids	39
4.2.2 Anthocyanin	42
4.3 Photosynthesis	44
4.3.1 Light Responses	44
4.3.1.1 Photosynthetic Derived Parameters at 200 C _a	47
4.3.1.2 Photosynthetic Derived Parameters at 400 C _a	50
4.3.1.3 Photosynthetic Derived Parameters at 800 C _a	53
4.3.1.4 Intrinsic Water Use Efficiency.....	55
4.3.2 CO ₂ Responses	55
4.4 Photoinhibition of Photosynthesis	60
5.0 DISCUSSION	62
5.1 Responses to Growth Irradiance	62

5.1.1 Shandong: A Tough Resilient Plant	62
5.1.2 Yukon: A High-light Loving Plant	64
5.2 Contrasting Results between Ecotypes Acclimated to High-Light	66
5.3 Conclusions and Future Work	67
6.0 REFERENCES	69

LIST OF TABLES

<u>Table</u>	<u>Page</u>
Table 4.1	Relative growth rates (RGR) for the Shandong and Yukon ecotypes of <i>Eutrema</i> developed at different growth irradiance37
Table 4.2	Leaf chlorophyll and carotenoid contents for the Shandong and Yukon ecotypes of <i>Eutrema</i> developed at different growth irradiance41
Table 4.3	Leaf anthocyanin content for the Shandong and Yukon ecotypes of <i>Eutrema</i> developed at different growth irradiance43
Table 4.4	Photosynthetic parameters derived from light-response curves at 200 C_a of the Shandong and Yukon ecotypes of <i>Eutrema</i> grown under two different irradiance49
Table 4.5	Photosynthetic parameters derived from light-response curves at 400 C_a of the Shandong and Yukon ecotypes of <i>Eutrema</i> grown under two different irradiance52
Table 4.6	Photosynthetic parameters derived from light-response curves at 800 C_a of the Shandong and Yukon ecotypes of <i>Eutrema</i> grown under two different irradiance54
Table 4.7	Intrinsic water use efficiency of the Shandong and Yukon ecotypes of <i>Eutrema</i> grown under under two different irradiance56
Table 4.8	Photosynthetic parameters derived from CO ₂ -response curves of Shandong and Yukon ecotypes grown under two different irradiance58

LIST OF FIGURES

<u>Figure</u>		<u>Page</u>
Figure 2.1	General diagram of light and carbon reactions of photosynthesis	5
Figure 2.2	Main reactions of the photorespiratory pathway	10
Figure 2.3	Diagrammatic representation of photostasis	12
Figure 4.1	Fresh weight (FW) accumulation for the Shandong and Yukon ecotypes of <i>Eutrema</i> developed at different growth irradiance	27
Figure 4.2	Dry weight (DW) accumulation for the Shandong and Yukon ecotypes of <i>Eutrema</i> developed at different growth irradiance	28
Figure 4.3	Total leaf area (LA) for the Shandong and Yukon ecotypes of <i>Eutrema</i> developed at different growth irradiance	29
Figure 4.4	Number of accumulated leaves for the Shandong and Yukon ecotypes of <i>Eutrema</i> developed at different growth irradiance	31
Figure 4.5	Leaf relative water content for the Shandong and Yukon ecotypes of <i>Eutrema</i> developed at different growth irradiance	32
Figure 4.6	Fresh weight to dry weight ratio (FW:DW) for the Shandong and Yukon ecotypes of <i>Eutrema</i> developed at different growth irradiance	33
Figure 4.7	Specific leaf area (SLA) for the Shandong and Yukon ecotypes of <i>Eutrema</i> developed at different growth irradiance	35

Figure 4.8	Phenotypic comparisons for the Shandong and Yukon ecotypes of <i>Eutrema</i> developed at different growth irradiance	38
Figure 4.9	Light-response curves at 200 C_a for the Shandong and Yukon ecotypes of <i>Eutrema</i> developed at different growth irradiance	45
Figure 4.10	Light-response curves at 400 C_a for the Shandong and Yukon ecotypes of <i>Eutrema</i> developed at different growth irradiance	46
Figure 4.11	Light-response curves at 800 C_a for the Shandong and Yukon ecotypes of <i>Eutrema</i> developed at different growth irradiance	48
Figure 4.12	CO ₂ -response curves for the Shandong and Yukon ecotypes of <i>Eutrema</i> developed at different growth irradiance	57
Figure 4.13	Photoinhibition of photosynthesis for the Shandong and Yukon ecotypes of <i>Eutrema</i> developed at different growth irradiance	61

LIST OF ABBREVIATIONS

$\Phi_{\text{app CO}_2}$	Apparent quantum yield of CO ₂ uptake
Γ^*	CO ₂ compensation point
σ_{PSII}	Effective absorption cross-section of PSII
E_k	Irradiance at which the photosynthetic electrons are consumed by terminal electron acceptors
τ^{-1}	Rate of electron consumption
2-PG	2-phosphoglycolate
3-PGA	3-phosphoglycerate
A_{max}	maximal rate of net photosynthesis (at saturating CO ₂ or irradiance)
ANOVA	Analysis of variance
ATP	Adenosine triphosphate
C_a	Ambient CO ₂ ($\mu\text{mol mol}^{-1}$)
CE	Carboxylation efficiency
Chl	Chlorophyll
Cyt	Cytochrome
D1	One of the proteins of PSII core heterodimer
DW	Dry weight
ETC	Electron transport chain
Fd	Ferredoxin
F_m	Maximal fluorescence in the dark-adapted state

F _o	Minimal fluorescence in the dark-adapted state
F _v /F _m	Maximum quantum efficiency of PSII photochemistry
FW	Fresh weight
HL	High light
IRGA	infra-red gas analysis
LA	Leaf area
LHCI	Light harvesting complex I
LHCII	Light harvesting complex II
LL	Low light
LSE	Light saturation estimate
NADP ⁺	Nicotinamide adenine dinucleotide phosphate – oxidized form
NADPH	Nicotinamide adenine dinucleotide phosphate – reduced form
NPQ	Non-photochemical quenching
P680	Primary electron donor of PSII
P700	Primary electron donor of PSI
PC	Plastocyanin
PPFD	Photosynthetic photon flux density
PQ	Plastoquinone
PQH ₂	Plastoquinol
PsbS	Photosystem II subunit S
PSI	Photosystem I

PSII	Photosystem II
PTOX	Plastid terminal oxidase
Q _A	Primary quinone electron acceptor of PSII
Q _B	Secondary quinone acceptor
q _E	Energy dependant quenching
R _{dark}	Rate of dark respiration
RC	Reaction centres
RGR	Relative growth rate
ROS	Reactive oxygen species
Rubisco	Ribulose-1,5-biphosphate carboxylase/oxygenase
RuBP	Ribulose-1,5-biphosphate
RuP	Ribulose monophosphate
SD	Standard deviation
SE	Standard error
SLA	Specific leaf area

CHAPTER 1

1.0 Introduction

Eutrema salsugineum (Pall.) Al-Shehbaz and Warwick is a model plant for research on stress tolerance (Bressan et al. 2001; Inan et al. 2004; Wong et al. 2005; 2006). This plant is closely related with the model plant *Arabidopsis thaliana* and both belong to the Brassicaceae family. As *Arabidopsis* and *Eutrema* are similar there is an advantage to use techniques developed for *Arabidopsis* in *Eutrema* (Amtmann 2009). The Brassicaceae family has been subjected to taxonomic reclassification as new molecular and phylogenetic techniques appear. A lack of integration between disciplines lead to some erroneous names and re-grouping (Koch and German 2013). Amtmann (2009) pointed out some of the taxonomic erroneous classification as well. Thus, *Eutrema salsugineum* can be found in the literature as *Thellungiella salsuginea* and/or incorrectly as *Thellungiella halophila*. Some studies classified *Eutrema* as an extremophile plant owed to its capacity to grow and reproduce under extremely harsh conditions of cold (Griffith et al. 2007; Khanal et al. 2015), salinity (Bressan et al. 2001; Inan et al. 2004; Taji et al. 2004) drought (Wong et al. 2005) and poor nutrient availability (Kant et al. 2008). Two main ecotypes have been used in abiotic stress studies. The Shandong ecotype from the Shandong province in North-Eastern China grows naturally in high-salinity coastal areas for that reason is considered a halophyte plant and with day lengths of 14 hours in the summer (Inan et al. 2004; Taji et al. 2004; Amtmann et al. 2005; Orsini et al. 2010; Yang et al. 2013). The Yukon ecotype from the Yukon Territory in Northwest Canada, grows in a semi-arid, subarctic region with low nitrogen content in the soil (Guevara et al. 2012) with day lengths as long as 21 hours in the summer (Griffith et al. 2007). This research aims to assess the photoacclimation mechanisms of two ecotypes of the extremophilic model plant *Eutrema* to different growth irradiance levels. Plants were grown under controlled conditions with LL and HL, other parameters were based on the Yukon regime (Griffith et al. 2007).

Plants can photoacclimate because photosynthesis itself is a dynamic process that can act as a sensor mechanism and maintain a photostasis under prevailing growth conditions. Photoacclimation prevents light-limitation under low and photoinhibition under high irradiance (Aro et al. 1993; Anderson et al. 1995; Huner et al. 1998). To

assess the photoacclimation mechanisms of these two ecotypes at LL and HL growth irradiance, growth kinetics, gas exchange measurements, pigment determination and tolerance to photoinhibition of photosynthesis were studied.

The majority of studies done on *Eutrema* have assessed salinity tolerance. However, there is a lack of research studying photosynthesis as a stress sensor and the responses to HL and the photoacclimation mechanisms of these plants to different growth irradiance (Wong et al. 2006; Stepien and Johnson 2009; Sui and Han 2014).

A combination of multiple stress conditions can seriously affect plant growth and productivity and one of the most important environmental stresses can be exposure to high irradiance. The exposure to light levels in excess of the plants capacity to utilize this energy for metabolic processes results in a decrease in the rate of photosynthesis. Therefore, stress tolerant crops should be developed to maintain high crop yields, a further understanding of the mechanisms of photoacclimation of the extremophile plant *Eutrema salsugineum* can provide more information to develop stress tolerant crop plants.

1.1 Hypothesis and Objectives

1.1.1 Hypothesis

The Shandong and Yukon ecotypes of *Eutrema salsugineum* exhibit different photoacclimation mechanisms to growth irradiance that reflects adaptation to contrasting environments.

1.1.2 Overall Objective

The general objective of this project was to elucidate and examine the photoacclimation mechanisms of the Shandong and Yukon ecotypes of *Eutrema salsugineum* to LL and HL growth regimes.

1.1.3 Specific Objectives

- To assess growth and development of the Shandong and Yukon ecotypes of *Eutrema* under LL and HL regimes.

- To determine changes in photosynthetic pigments of *Eutrema* in response to photoacclimation to LL and HL regimes.
- To study photosynthetic and photoinhibitory responses of the Shandong and Yukon ecotypes in response to photoacclimation to LL and HL conditions.

To achieve the above objectives, this study covers growth and development, pigment determination and photosynthesis of the Shandong and Yukon ecotypes of *Eutrema* under LL and HL regime with the same conditions of temperature, and photoperiod. Results are presented as described below. First a growth kinetics experiment compares different growth parameters of the two ecotypes across the different growth irradiance. The second main topic assesses photoacclimation of the two ecotypes in response to low and high-light determining the differential response in the photosynthetic pigments. And finally, a photosynthetic determination done to assess CO₂ and light responses of the two ecotypes grown under LL and HL to study the photoacclimation mechanisms of these two ecotypes including photosynthesis, photorespiration and tolerance to photoinhibition.

CHAPTER 2

2.0 Literature Review

2.1 *Photosynthesis*

All life on earth depends directly or indirectly on the energy provided by the sun. Photosynthesis is a biochemical mechanism that allows the photosynthetic organisms to harvest this energy and transform it to usable forms. This process is similar in all photosynthetic organisms with subtle variations and involves a complex series of reactions and can be divided mainly in two phases: light reactions and carbon reactions (Malkin and Niyogi 2000; Lawlor 2001). The process is represented graphically in Fig. 2.1. The light reactions yield O₂, ATP, and NADPH through photosynthetic electron transport and is regulated by proton gradient within the thylakoid (Hüner and Grodzinski 2011). The carbon reactions or Calvin cycle, reduces CO₂ to carbohydrate and uses the ATP and NADPH produced in the light reactions. The photosynthetic process takes place in the chloroplasts in the thylakoid membrane (Ensminger et al. 2006).

2.1.1 *Light Reactions*

The process starts when light is absorbed by pigments that are located in pigment-protein complexes within the thylakoid. These complexes form a photosystem (PS), each PS is constituted by about 250 Chl molecules. Most of these chlorophyll molecules form the antenna. LHCs are divided according to the photosystem that they are associated. LHCI is associated with PSI and LHCII with PSII. The reaction centres (RC) are inside the core complex. Only special forms of Chl *a* can form RC. The other type of pigments are accessory and form arranged groups of light-capturing units acting as antennae to capture photons (Lawlor 2001). The energy absorbed by the antennae is transferred to the reaction centers of PSI and PSII (Croce and van Amerongen 2013).

The RC are part of the electron transfer chain that connects the two photosystems and also where the light energy is transformed into chemical energy. RC can be divided according to the chemical nature of the electron acceptors. PSII has a quinone type acceptor also known as Q-type and PSI has an iron-sulfur acceptor also known as Fe-S type acceptor (Caffarri et al. 2014). The PSII reaction centre is a multisubunit protein supercomplex that is integral in the thylakoid membrane. The PSII

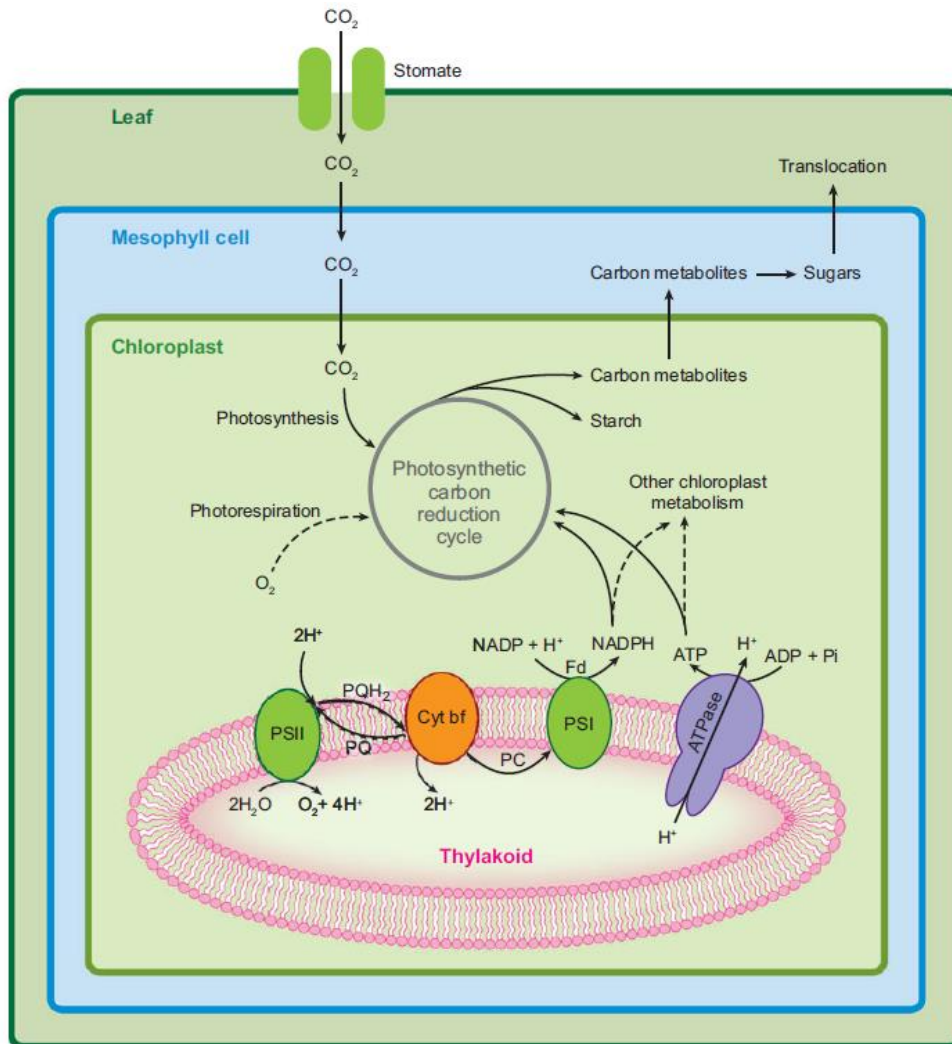


Figure 2.1 General diagram of light and carbon reactions of photosynthesis (from Baker 2008). Cyt *bf*, cytochrome *b₆f* complex; Fd, ferredoxin; PC, plastocyanin; PQ plastoquinone; PQH₂, plastoquinol; PSI, photosystem I; PSII, photosystem II; Rubisco, ribulose 1,5-biphosphate carboxylase/oxygenase; RuBP, ribulose 1,5-biphosphate.

The excitation energy provided by the sun causes a charge separation in the PSII RC, this energy is used to drive photochemistry and the linear electron transport begins at P680. The excited P680* donates an electron to pheophytin that forms a P680⁺ and pheophytin⁻, this charge separation is known as photo-oxidation when an electron is transferred from P680 to Q_A that is bound to the D1 reaction centre, P680⁺ is a strong oxidant and accepts an electron from water of the oxygen evolving complex (Minagawa and Takahashi 2004). Q_A is the first stable quinone acceptor to produce a plastoquinone Q_A⁻. The electron then is transferred to the second quinone acceptor Q_B that is bound to the D2 reaction center polypeptide and generates the semiquinone Q_B⁻. (Malkin and Niyogi 2000; Hüner and Grodzinski 2011). A second electron can be accepted by the quinones and a fully reduced Q_B²⁻ can be associated with two protons from the stromal side of the membrane and produce a plastoquinol Q_BH₂, after reduction and protonation this molecule leaves the PSII reaction centre complex to the thylakoid membrane and functions as a mobile electron carrier. Q_BH₂ associates with Cyt b₆/f protein complex and transfers two electrons to the b₆/f complex and releases two protons into the thylakoid membrane creating an electrochemical difference between the thylakoid membrane and stroma (ΔpH) (Fig. 2.1) (Baker et al. 2007; Bowsher et al. 2008; Malkin and Niyogi 2000). The cytochrome b₆/f complex works as a plastoquinol-plastocyanin oxidoreductase and transfers electrons from plastoquinol to plastocyanin and connects the two photosystems. Simultaneously with the electron transfer there is a translocation of protons across the membrane that facilitates a formation of a proton gradient that drives ATP synthesis. The PSI reaction centre is similar to PSII but the special forms of Chl *a* are known as P700 and it is a heteromultimeric pigment-protein complex associated with a light-harvesting complex (LHCI) (Lawlor 2000). PSI complex functions as a light-dependent plastocyanin-ferredoxin oxidoreductase. The reduced plastocyanin binds the PSI and the absorbed excitation energy then transfers electrons from plastocyanin to ferredoxin. PSI reduces NADP⁺ to NADPH by the action of ferredoxin and flavoprotein ferredoxin-NADP reductase (Fig. 2.1). This flux of electrons called linear electron flux then is coupled to proton release at the oxygen evolving complex, transporting protons across the thylakoid membrane establishing a proton motive force that drives the synthesis of ATP through the chloroplast ATP synthase by

chemiosmotic coupling (Mitchell 1966; Malkin and Niyogi 2000; Lawlor 2001; Cruz et al. 2005). NADPH and ATP are later on used in the carbon reactions of photosynthesis to fix CO₂ (Wilson et al. 2006).

The energy absorbed through the photosynthetic apparatus has different fates; drive the photochemistry transferring electrons from the RC P680 to Q_A, as an alternative fate energy can be re-emitted as fluorescence by Chl *a*. Under normal circumstances, up to 3% of the absorbed light by chlorophyll molecules is re-emitted as fluorescence, or dissipated as heat by non-photochemical quenching (NPQ) (Horton et al. 2005; Wilson et al. 2006), changes in fluorescence yield are inversely correlated with the rate of photosynthetic electron transfer because these processes are in direct competition for excitation energy (Baker 2008; Eberhard et al 2008). All photosynthetic organisms exhibit chlorophyll *a* fluorescence, due to the photochemical properties of the molecule, and its role in the structure and function of the photosynthetic apparatus.

Chlorophyll fluorescence measurements provide a sensitive, rapid, non-invasive and non-destructive method to assess photosynthetic responses, particularly the light reactions. Generally a loss or decrease in the maximum quantum yield of PSII photochemistry (F_v/F_m) is a reliable indicator of abiotic stress, such as photoinhibition (Ögren 1991; Krause and Weis 1991).

2.1.2 Carbon Reactions

The ATP and NADPH produced in the light reactions of photosynthesis then are consumed in the carbon reactions to reduce CO₂ and produce a three-carbon compound, 3-phosphoglycerate (3-PGA) that is the first stable product of a multistep conversion of CO₂ into carbohydrate. This pathway is commonly known as the Calvin-Benson cycle. However, there are other metabolic pathways associated with photosynthetic fixation of CO₂ that are dependent or associated with the Calvin-Benson cycle as can be diagrammatically observed on Fig. 2.1 (Taiz and Zeiger 2006).

The Calvin-Benson cycle proceeds in three different stages and through 13 steps: carboxylation of RuBP that forms a transient unstable six-carbon intermediate that remains attached to the enzyme then is hydrolyzed and yields two molecules of 3-PGA. This reaction is catalyzed by the enzyme ribulose-1,5-biphosphate

carboxylase/oxygenase (Rubisco). Rubisco activity is apparently activated indirectly by light. Rubisco activase is a light-dependent enzyme that uses free energy from ATP hydrolysis ensuring that the active sites are available (Perchorowicz et al. 1981). The electron transport chain from the light reactions leads to a movement of protons that creates a gradient across the thylakoid membrane that increases pH of the stroma from around 5.0 in the dark up to 8.0 in the presence of light (Hopkins and Hüner 2004). Light also is responsible for an increase in the free Mg^{2+} that helps with the stabilization of the carbamate during the carbamylation process (Stec 2012). The former described steps are required in the presence of light for the activation of Rubisco. The reduction of 1,3-biphosphoglycerate by NADPH to glyceraldehyde 3-phosphate is catalyzed by glyceraldehyde 3-phosphate dehydrogenase. NADPH is oxidized to $NADP^+$. The following step is regeneration of RuBP that allows the Calvin cycle to continue. Triose phosphate isomerase converts all the glyceraldehyde 3-phosphate into dihydroxyacetone phosphate, this reaction is catalyzed by the enzyme aldolase. The following step in the regeneration is the hydrolysis of fructose 1,6-biphosphate. This reaction is catalyzed by the enzyme fructose 1,6-biphosphatase and yields fructose 6-phosphate. Transketolase removes two carbons from fructose 6-phosphate and add them to glyceraldehyde 3-phosphate producing xylulose 5-phosphate and erythrose 4-phosphate. The enzyme aldolase forms sedoheptulose 1,7-biophosphate and transketolase removes two-carbons from sedoheptulose 7-phosphate and transfers them to glyceraldehyde 3-phosphate to produce 5-phosphate and xylulose 5-phosphate. Ribulose 5-phosphate is formed from xylulose 5-phosphate by ribulose 5-phosphate epimerase, and ribose 5-phosphate by ribose 5-phosphate isomerase. The last step phosphoribulokinase phosphorylates RuP into RuBP, this is an irreversible reaction and consumes one ATP (Bowsher et al. 2008).

Rubisco is able to act as oxygenase using the same substrate RuBP binding oxygen instead of carbon dioxide inhibiting the carboxylase reaction and beginning the photorespiration pathway (Hagemann et al. 2013). The products of this reaction are one molecule of 3-phosphoglycerate and 2-phosphoglycolate (Timm et al. 2012). 3-PGA can be integrated later on to the Calvin-Benson cycle. 2-PG and its derivatives glycolate and glyoxylate eventually are recycled into 3-PGA leading to a loss of carbon and nitrogen

(Ros et al. 2013). The enzyme Rubisco has a lower affinity for oxygen than to carbon dioxide, thus photorespiration is favoured under conditions of low CO₂ or high O₂ (Timm and Bauwe 2013).

2.2 Photorespiration

The photorespiratory pathway takes place in three organelles with more than 15 enzymes and translocators being involved (Lawlor 2001). This is shown diagrammatically in Fig. 2.2. Photorespiration starts in the chloroplast with the oxidation of RuBP that yields one 3-PGA and one 2-PG that is dephosphorylated to glycolate through 2-phosphoglycolate phosphatase (Maurino and Peterhansel 2011). Later on glycolate diffuses to the peroxisome. In the peroxisome the glycolate derived from 2-PG reacts with O₂ this reaction is catalyzed by the enzyme glycolate oxidase and yields glyoxylate and H₂O₂. Hydrogen peroxide produces H₂O and O₂ by catalase. The glyoxylate is converted into two molecules of glycine by an aminotransferase reaction. In the mitochondrion the two glycine molecules are metabolized through a series of complex reactions by the enzymes glycine decarboxylase complex and serine hydroxymethyl transferase. These reactions produce carbon dioxide, ammonia, NADPH and lead to the formation of serine. This compound moves to the peroxisome by an aminotransferase reaction and is converted to hydroxypyruvate, reduced to glycerate via an NADPH-dependent reductase. NADPH is transferred from the cytoplasm to the peroxisome by a malate-oxaloacetate shuttle, and subsequently returned to the chloroplast to be converted to 3-PGA and re-enter the Calvin cycle (Taiz and Zeiger 2006). Photorespiration has been considered as a wasteful process in plants, but recent studies (Maurino and Peterhansel 2010; Bauwe et al. 2012) have shown that the photorespiratory pathway is an integral element of primary carbon metabolism which interacts with other pathways. Wingler et al. (2000) suggests that photorespiration is a beneficial process that supports growth under stress conditions. Huang et al. (2014) reported that tobacco leaves exposed to high irradiance have an improved photorespiratory pathway that enables to speed up the recycling of 2-PG to 3-PGA as a result there is a regulation in the balance between RuBP oxygenation and regeneration that helps modulating the RuBP content in chloroplasts. As a final finding

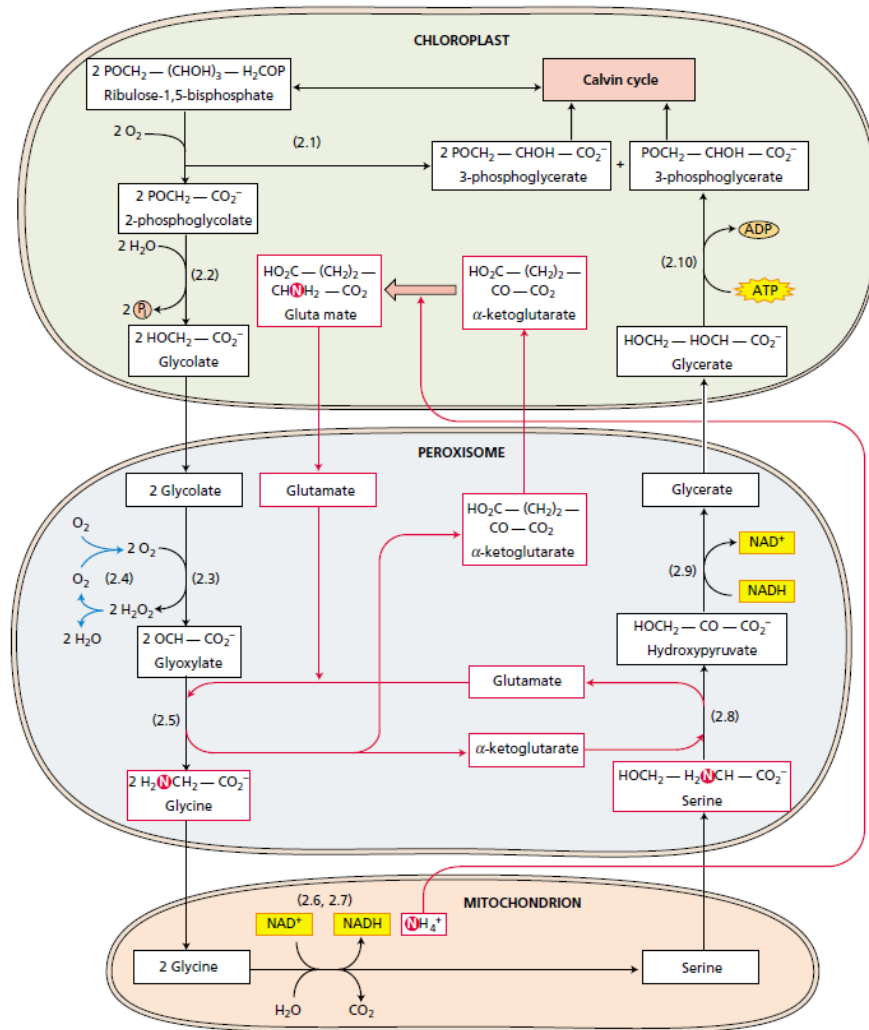


Figure 2.2 Main reactions of the photorespiratory pathway. This process takes place in the chloroplast, peroxisome and mitochondrion (From Taiz and Zeiger 2006). ADP, adenosine diphosphate; ATP, adenosine triphosphate; NADH, nicotinamide adenine dinucleotide.

they suggest that the enhancement of the photorespiratory pathway is essential for HL plants to maintain high photosynthetic rates. Timm et al. (2012) demonstrated with mutant plants of *Arabidopsis* that the overexpression of glycine decarboxylase considerably can increase the net rate of photosynthesis and that a close interaction exists between the photorespiratory and the Calvin cycle.

2.2 Photostasis

Photosynthetic organisms have a predisposition to maintain a balance between energy captured by the photochemical reactions and the energy used through biochemical reactions, balancing energy sources and sinks (Wilson et al. 2006; Murchie et al. 2009). This energy balancing is called photostasis (Öquist and Hüner 2003; Ensminger et al. 2006). Energy balance is represented by the equation $\sigma_{\text{PSII}} \times E_k = \tau^{-1}$ (Falkowski and Chen 2003), where σ_{PSII} is the effective cross-section absorption of PSII, E_k is the irradiance at which the photosynthetic electrons are consumed by terminal electron acceptors. σ_{PSII} is temperature insensitive within the biological significant range. Conversely, τ^{-1} is highly sensitive to temperature (Wilson et al. 2006; Hüner et al. 2013). When a metabolic sink cannot work at the same speed as the utilization of the absorbed energy plants need to use balancing mechanisms to reestablish photostasis (Ensminger et al. 2006). To restore photostasis the plant needs to readjust the flow of energy by decreasing the rate of energy in the source adjusting the cross section of PSII, balancing the excess of photons via NPQ, modulating the light harvesting complex associated with PSII, decreasing the incident irradiance or increasing the sink processes that are determined primarily by carbon and nitrogen metabolism or combining various of these mechanisms to rebalance energy (Hüner et al. 1998, 2003; Ensminger et al. 2006; Biswal et al. 2011). This process can be diagrammatically observed on Fig. 2.3. Low temperature and high irradiance can cause an over-acidification of the lumen and over-reduction in the redox status of the photosynthetic electron carriers, these mechanisms act as physiological indicators of high excitation pressure of PSII that can lead to photoinhibition if the energy source exceeds the sinks capacity (Ensminger et al. 2006; Wilson et al. 2006; Derks et al. 2015).

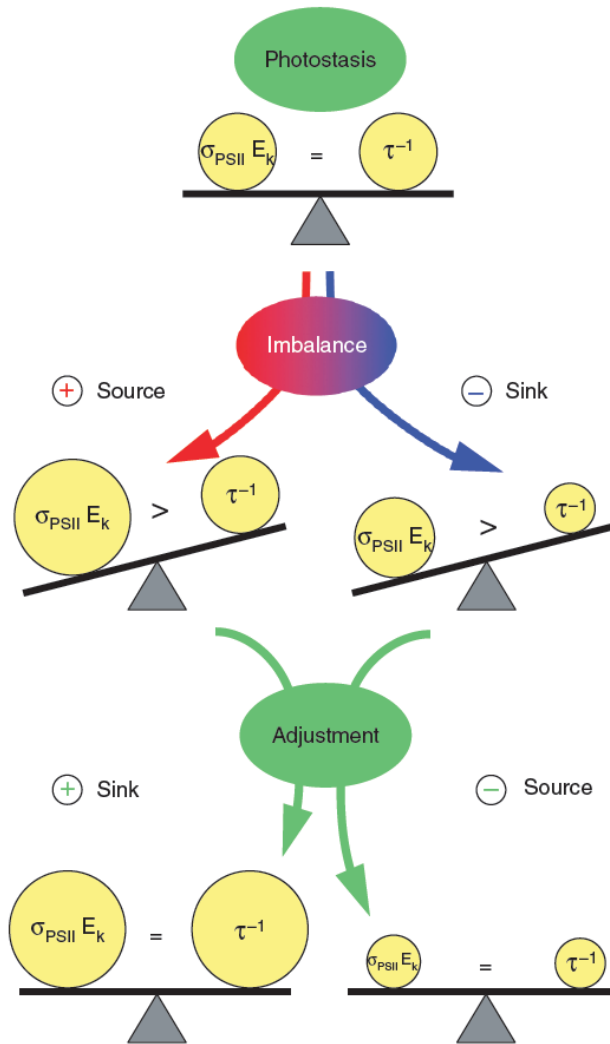


Figure 2.3 Diagrammatic representation of photostasis. Photosynthetic adjustment is made to achieve photostasis when an imbalance is sensed. To balance the energy again plants increase the sink processes, decrease the rate of incoming energy or both (From Ensminger et al. 2006). σ_{PSII} , effective cross-section absorption of PSII; τ^{-1} , rate of electron consumption; E_k , irradiance at which the photosynthetic electrons are consumed by terminal electron acceptors.

Photoinhibition can be defined as a temporary decrease of the photosynthetic rates during stressful environmental conditions the reaction centre of PSII is inactivated and sometimes damaged (Melis 1999). Low temperature does not affect the light absorption but it slows down the enzyme-catalyzed reactions causing an over-reduction of PQ by creating an imbalance between sources and sinks. Therefore, low temperature and high Irradiance generally trigger photoinhibition decreasing the photosynthetic rates and photosynthetic activity of PSII (Gray et al. 2003). Photoinhibition can be chronic as a result of an exposure to excess of light. Under these conditions quantum efficiency and maximum photosynthetic rates are decreased and can be associated with the damage of the D1 protein of the reaction centre of PSII (Taiz and Zeiger 2006). PSII can transfer excitation energy from chlorophyll to oxygen if there is a time lag in photochemical energy transformation causing an accumulation of reactive singlet oxygen. In a similar way if NADP is unable to accept electrons from PSI from the electron transport chain it may reduce oxygen to the superoxide radical or transfer electrons to water to form the hydroxyl radical and hydrogen peroxide. These compounds are known as reactive oxygen species and play an important role in cellular signalling. However, ROS can potentially cause oxidative damage to nucleic acids, proteins and lipids (Demmig-Adams and Adams III 2000; Eberhard et al. 2008; Ruban 2009; Vishwakarma et al. 2014).

Plants have evolved different mechanisms of photoprotection and these mechanisms can be classified depending on the time scale in the change of the environmental conditions. To avoid irreversible photodamage plants have ROS scavenging mechanisms, carotenoids are able to scavenge the triplet excited state of chlorophyll and singlet oxygen when triplet chlorophyll increases because a lag in the photochemistry of the plant is present (Carbonera et al. 2005; Eberhard et al. 2008). The photoprotective mechanisms help the plant to achieve again a photostatic balance and can be classified as photochemical that are mainly electron sinks and non-photochemical (Murchie et al. 2015). Non-photochemical quenching refers to the thermal dissipation of an excess of energy in PSII (Horton and Ruban 2005; Belgio et al. 2014). qE is one of the main forms of NPQ and is activated by the acidification of the thylakoid lumen and is induced after an exposure to high light (Avenson et al. 2004).

The thylakoid acidification induces a change in the protonation of the PSII proteins that contributes to dissipate the excess of energy (Ruban et al. 2012). Protonation activates the xanthophyll cycle and triggers a reaction that is catalyzed by the enzyme violaxanthin de-epoxidase the de-epoxidation of the xanthophyll violaxanthin via anteraxanthin to zeaxanthin (Arnoux et al. 2009). Other important component of NPQ is the PsbS protein and was discovered screening *Arabidopsis* mutants with altered chlorophyll fluorescence quenching, PsbS is involved in the formation of qE (Li et al. 2000). Mutant plants of *Arabidopsis* defectives in PsbS encoding for qE were more susceptible to photoinhibition under high irradiance (Li et al. 2002; Niyogi et al. 2005).

Plants can balance the distribution of excitation energy between the two photosystems through state transitions this mechanism helps to maximize the efficiency of the light harvesting under low irradiance (Allen and Forsberg 2001; Mullineaux and Emlin-Jones 2005). However, Lunde et al. (2003) found that state transitions does not appear to play an important role in *Arabidopsis* optimizing photosynthesis under low light conditions or as a protective strategy under high irradiance.

The Mehler-Asada cycle scavenges the superoxide radicals formed from the splitting of water molecules at the oxygen evolving complex of PSII are transferred to oxygen (Asada 1999, 2000). The plastid terminal oxidase (PTOX) builds-up a proton motive force across the thylakoid membrane releasing water on the stromal side of the membrane accepting electrons from plastoquinol and reducing O₂, PTOX has been demonstrated as a safety valve but typically is more abundant and active in young leaves (Peltier and Cournac 2002; Shirao et al. 2013). However, Stepien and Johnson (2009) reported a high capacity of PTOX under salt stress in mature leaves of *Eutrema* (*Thellungiella halophila*). The malate valve works to avoid an over-reduction of the ETC and chloroplast stroma exporting to the cytosol and mitochondria the excess of equivalents produced in the chloroplast (Scheibe 2004). A controlled oxidative damage in the plant compartmentalized can protect the rest of the photosynthetic apparatus as the D1 protein that is considered a “suicide protein” (Aro et al. 1993). Turnover of the D1 protein is highly regulated and allows the plant to continue photosynthesizing under stress conditions. D1 suffers photooxidative damage then a reversible phosphorylation of several PSII core units, followed by a dissociation of LHCII supercomplexes, PSII

complex dimmers are monomerized, the monomers move to the stromal thylakoids from the granal stacks, finally there is a partial disassembly of the PSII core monomer and the damaged D1 protein is ubiquitinated (Aro et al. 2005; Mulo et al. 2008; Tikkanen et al. 2013). Photorelocation does not involve any change in the stoichiometry of the photosynthetic machinery, instead there is a chloroplast movement as part of a light avoidance response (Kasahara et al. 2002; Morita and Nakamura 2012). Modifying the leaf angle allows the plants to reduce the light absorption to decrease the source of energy and maintain photostasis (Murchie et al. 1999).

2.3 Photoacclimation

As mentioned before, the natural environment where plants grow possess a high variability that represents a challenge for the plants because they have to compete with others plants for light, water and nutrients and at the same time cope with biotic and abiotic stress (Hirth et al. 2013; Walters 2005). Plants have developed different mechanisms to sense the environment. When an imbalance alters the physiological homeostasis there is a readjustment to achieve again the homeostatic conditions activating cellular, physiological, and developmental changes acclimating within hours or days to optimize growth and reproductive capacity. Depending on the time scale of the change in the environmental conditions plants can use acclimation or adaptation if any alteration in the genetic material is involved (Hüner 1993; Walters 2005). According to Wilson et al. (2006) photoacclimation can be defined as any process that affects cellular energy balance that induces changes in the structure and function of the photosynthetic apparatus in response to growth changes.

If the plant is not able to cope with the environmental changes that causes the stress condition can lead to serious damage or be lethal (Gaspar et al. 2002; Jenks and Hasegawa 2005; Larkindale and Vierling 2008).

When plants are shifted from one growth irradiance condition to another, their capacity to adjust to the new conditions is often leaf-age dependent, mature leaves exhibit a lower degree of adjustment mainly due to morphological constraints as there is no possibility to alter the stomatal and vein density. As a result no up-regulation of

photosynthetic capacity can occur because of these morphological limitations (Adams et al. 2007).

Photoacclimation triggers a complex reorganization of the photosynthetic apparatus and consists of chloroplast level photoacclimation, leaf level photoacclimation and finally whole plant level photoacclimation (Murchie and Horton 1998; Bailey et al. 2001; Walters et al. 2003). At a chloroplast level photoacclimation involves changes in pigments composition, composition of the light harvesting antennas of PSI and PSII, Chl *a:b* ratio, Calvin cycle enzymes levels (Anderson and Osmond 1987; Anderson et al. 1995; Murchie and Horton 1998). When plants are grown under LL conditions the antenna sizes of PSI and PSII are larger, the opposite condition can be observed when plants are grown under HL conditions (Leong and Anderson 1984; Anderson and Osmond 1987). Changes in the stoichiometry of the two photosystems is typically observed as a result of the changes in the spectral quality of the light and no changes are observed for light growth intensities as Walters and Horton (1995) studied in *Arabidopsis*. PSII levels of wild type (WT) *Arabidopsis* plants was increased by 50% when plants were grown under HL conditions (Walters et al. 1999; Bailey et al. 2001). Leong and Anderson (1984) demonstrated on pea plants that LHCII decreases relative to PSII during growth at HL, this same results were obtained by Walters and Horton (1994) in *Arabidopsis*. The decrease in PSII antenna size might confer higher tolerance to photoinhibition as demonstrated by Park et al. (1997) in pea plants. The modification of the antenna sizes are reflected in the Chl *a:b* ratios, typically plants grown under low light intensities have lower *a:b* ratio than plants grown under high light (Anderson and Osmond 1987). Chl *a:b* ratio response is very clear in *Arabidopsis*. Pea plants exhibit the same response as *Arabidopsis* with increased ratios when plants are grown under high irradiance (Leong and Anderson 1984; Walters and Horton 1994). However, not all species exhibit the same response to Chl *a:b* ratio. Chow et al. (1991) found that *Tradescantia albiflora* does not modify this ratio when is grown under high irradiance.

An increase in the amount of Cyt *b₆f* complex, increased electron capacity and Rubisco contents are also observed as an acclimation mechanism in *Arabidopsis*, spinach and peas. These changes allow the plants to support higher rates of photosynthesis under HL, also these characteristics can lead to higher light

compensation points and higher light saturation points (Leong and Anderson 1984; Stitt 1986 Anderson and Osmond 1987; Bailey et al. 2001 Lake et al. 2002; Schlüter et al. 2003). The higher rates of photosynthesis reflects the increased capacity of CO₂ fixation via the carbon reactions of photosynthesis (Bailey et al. 2001). Anderson et al. (1999) found a 3-fold increase in maximal photosynthetic rates when wild type plants of *Arabidopsis* were grown under HL conditions. Leaf level photoacclimation shows that plants grown under low-light have thinner leaves, whereas plants grown under high-light have thicker leaves and more columnar mesophyll cells. For instance, *Arabidopsis* plants modify leaf morphology with thicker leaves, shorter petioles and a more defined rosette formation for plants grown under high irradiance (Anderson and Osmond 1987; Bailey et al. 2001; Oguchi et al. 2003; Yano and Terashima 2004).

2.4 *Eutrema salsugineum*

Eutrema salsugineum (Pall.) Al-Shehbaz and Warwick is closely related with the model plant *Arabidopsis thaliana* and both belong to the Brassicaceae family. There are numerous plants from this family with economic value (Frankze et al. 2009), also this family is a widely distributed group of plants and they can grow under different stressful conditions displaying environmental adaptation (Bressan et al. 2001). Plant productivity can be seriously affected due to abiotic stresses, and studying plants that naturally possess a degree of resistance to harsh environmental conditions can lead to an improvement in plant production (Griffith et al. 2007). *Eutrema salsugineum* can be found in the literature as *Thellungiella salsuginea* and/or *Thellungiella halophila*.

Eutrema or salt cress is a model plant for research on stress tolerance (Bressan et al. 2001; Inan et al. 2004; Wong et al. 2005; 2006). Some studies classified *Eutrema* as an extremophilic plant (Wong et al. 2005; 2006; Amtmann, 2009) due to the capacity to grow and reproduce under extremely harsh conditions of cold, salinity drought and poor nutrient availability (Bressan et al 2001; Inan et al. 2004; Taji et al. 2004; Amtmann et al. 2005; Griffith et al. 2007; Kant et al. 2008; Amtmann et al. 2009; Guevara et al. 2012; Khanal et al. 2015).

Two ecotypes of *Eutrema* have been used in abiotic stress studies; the Shandong ecotype from the Shandong province in China (37°16'12"N 118°18'0" E) that

grows naturally in high-salinity coastal areas. This ecotype has proven to be very tolerant to high salt concentrations in the soil and for that reason is considered a halophyte (Inan et al. 2004; Taji et al. 2004; Amtmann et al. 2005; Orsini et al. 2010; Yang et al. 2013). The Yukon ecotype from the Yukon Territory in Northwest Canada (60°51'17"N 135°43'2"W), grows in a semi-arid, subarctic region (Guevara et al. 2012).

The majority of studies done on *Eutrema* have assessed salinity tolerance and not much research has been done studying photosynthesis as a stress sensor and the responses to high-light and the photoacclimation mechanisms of these plants to different growth irradiances (Wong et al. 2006; Stepien and Johnson 2009; Sui and Han 2014).

CHAPTER 3

3.0 Materials and Methods

3.1 Plant Materials and Growth Conditions

The seeds of the Shandong and Yukon ecotypes (Shandong ecotype, stock no. CS22504 and Yukon ecotype, stock no. CS22664) obtained from Arabidopsis Biological Resource Centre (ABRC, The Ohio State University, Columbus, OH, USA) of *Eutrema salsugineum* (Pall.) Al-Shehbaz and Warwick were stored at 4°C, and germinated in small (63.5 mm) pots (Kord Products, Toronto, ON, Canada) containing Sungrow Sunshine LG3 soil medium (Sun Gro Horticulture Canada Limited, Seba Beach, AB, Canada). The medium was placed on a container and watered until it reached field capacity and pots were filled to the top. 3 to 4 seeds were planted per pot approximately 1 mm below the soil surface using a damp plastic tag. Pots were placed in a plastic tray with a capacity of 32 pots and a plastic cover was used to preserve humidity. Seven days after seeding the plastic cover was removed. Ten days after seeding the seedlings were thinned to 1 seedling per pot. Plants were grown in controlled environment chambers (Convion Model E8H, Controlled Environments Limited, Winnipeg, MB, Canada) in the University of Saskatchewan Phytotron. Growth conditions were 22/10°C (light/dark) temperature with a photoperiod of 21/3 hours (light/dark). Fluorescent tubes (Sylvania, T5/HO/841) provided 2 different photosynthetic flux density (PPFD) described as LL (250 $\mu\text{mol photons m}^{-2} \text{s}^{-1}$) and HL (750 $\mu\text{mol photons m}^{-2} \text{s}^{-1}$). Irradiance was determined at leaf level using a light meter (LI-250; Li-Cor Biosciences, Lincoln, NE, USA). Plants were irrigated regularly with a mineral nutrient solution described by Somerville and Ogren (1982). The growth conditions used were established previously for Yukon ecotype in Griffith et al. (2007).

3.2 Growth Analyses

3.2.1 Absolute Growth Parameters

The aerial portions of plants were harvested on a single plant basis and the fresh weight (FW) and leaf area was determined and number of leaves was recorded. Samples were placed in aluminum foil that has been previously weighed (NewClassic MF, model MS204S; Mettler Toledo, Langacher, Greifensee, Switzerland) and dried in

a drying oven (Model 70; Labco, Lucknow, India) on a single plant basis for a minimum of 48 hours at 90°C or until constant weight was obtained for the determination of dry weight (DW), subtracting the weight of the aluminum foil. Leaf water content (%) was estimated as $((FW-DW)/FW) \times 100$. For leaf area (LA) measurements a picture of the samples with 3 biological replicates per each sampling point was taken with a reference scale and analyzed with ImageJ freeware (National Institutes of Health, USA). The sampling points were determined for each growing chambers as follows: LL conditions after day 15 of seeding a sample was taken every 4 days until day 31. For the HL growing chamber after 15 days of seeding samples were taken every 3 days up to day 30.

3.2.2 Relative Growth Parameters

Relative growth parameters were derived from the absolute growth parameters. Specific leaf area (SLA) was calculated as LA/DW, this measurement calculates leaf area per unit of dry mass (Beadle 1993). Relative growth rate (RGR) was estimated on a dry weight basis and is defined as an increase in dry weight over time and is calculated as $RGR = (\ln DW_2 - \ln DW_1)/(t_2 - t_1)$. RGR was calculated over the whole life cycle of the plants. All measurements were done at the days indicated for each growing chamber which ensured the plants were at a comparable physiological stage (Boyes et al. 2001).

3.3 Photosynthetic Gas Exchange Measurements

In situ CO₂ exchange measurements were conducted using a Li-Cor portable photosynthesis system (LI -6400XT, Li-Cor). It is an open system; measurements of photosynthesis and transpiration are based in CO₂ and H₂O differences. The gas analyzer was calibrated daily and the start-up routine followed as described by the manufacturer. The net rate of CO₂ uptake (A_{max}) was determined using the whole plant chamber (WPA 6400-17, Li-Cor) which allows for whole plant gas exchange. The light source used for all the measurements was a LED RGB light source (LI-6400-18A; Li-Cor). White light was used and is comprised of equal proportions of red, green and, blue. After turning on the equipment, a new CO₂ cartridge (Crosman Corporation, USA)

was placed in the CO₂ mixer/injector and then calibrated setting the maximum level and then 10 different set points. CO₂ calibration allows that the infra-red gas analyzers (IRGA) warm up. Desiccant was replaced every day and soda lime (Alfa Aesar, Thermo Fisher Scientific, MA, USA) checked if it was able to absorb CO₂ giving a value close to zero on the device. CO₂ IRGA was checked for a proper zero adjusting the soda lime knob to full scrub and desiccant full bypass and flow set up to 500 $\mu\text{mol s}^{-1}$. If the difference between reference and sample was higher than 5 $\mu\text{mol mol}^{-1}$ the IRGAs required zeroing. IRGAs were zeroed when required only using new chemicals. H₂O IRGA was checked for a proper zero turning the desiccant to fully scrub until reading of the reference and sample was stabilized. If the difference between reference and sample was higher than 5 $\mu\text{mol mol}^{-1}$ the IRGAs required zeroing. For the IRGAs calibration the chamber must be empty and sealed. The chamber was sealed with an empty pot covered with plastic wrap (Glad ClingWrap; The Clorox Company of Canada, Brampton, ON) for a proper calibration. Leaf temperature thermocouple was calibrated disconnecting the thermocouple and matching block and leaf temperature on the screen with the adjusting screw located on the measuring head. Leaf fan functioning was also checked turning on and off the fan to listen for the sound change as the motor worked. After all the initial routine was done the CO₂ and H₂O IRGAs reference and sample sensors were matched to zero. Plants were irrigated with nutrient solution the day before measurements to avoid any potential water stress that leads to stomata closure thus, limiting gas exchange. All measurements were done with three technical replicates.

3.3.1 Light Responses

Light-response curves were obtained using a range of 0 to 1500 $\mu\text{mol photons m}^{-2} \text{s}^{-1}$ PPFD using a LED RGB light source (LI-6400-18A; Li-Cor). Measurements were made from high to low light intensity in 9 steps (1500, 1000, 750, 500, 250, 150, 100, 50 and 0 $\mu\text{mol photons m}^{-2} \text{s}^{-1}$) every step was maintained until stability was reached and then automatically changed to the next one. Light response curves were done with three different ambient CO_2 levels To accomplish this chamber reference CO_2 concentration was set at 200, 400 or 800 $\mu\text{mol mol}^{-1}$ (C_a) using a CO_2 mixer/injector (LI-6400-01; Li-Cor). Temperature was set at 22°C and fluctuated between 20.8 and 22.7°C and relative humidity fluctuated between 50 and 80% inside the measuring head. Gas exchange measurements were adjusted on leaf area basis, estimated through a scaled picture and calculated with ImageJ freeware (National Institutes of Health, USA).

Controls were done without plants to account for soil respiration. Pots with soil were kept under the same growth chamber as the plants and measured exactly as the plants sampled. Controls with only roots of the two ecotypes were done for each growth condition. The plants were grown as described on section 3.1 and before the measurements the aerial portion of the plant was trimmed. Results from both controls ranged from 0 to 1 $\mu\text{mol CO}_2 \text{ m}^{-2} \text{ s}^{-1}$ and were considered negligible.

3.3.1.1 Intrinsic Water Use Efficiency

Intrinsic water use efficiency (WUE) was calculated as A/E from each ecotype grown under two growth conditions. WUE was determined at an irradiance of 200 μmol and 800 photons $\text{m}^{-2} \text{s}^{-1}$ for LL and HL conditions, respectively. All measurements were determined from the light response curves done at 400 C_a .

3.3.2 CO_2 Responses

CO_2 -response curves were constructed at a saturating PPFD of 1500 $\mu\text{mol photons m}^{-2} \text{s}^{-1}$ using 8 different CO_2 chamber reference concentrations over the range of 0 to 1500 $\mu\text{mol mol}^{-1}$ in 8 steps (0, 50, 150, 250, 500, 750 and, 1500 $\mu\text{mol mol}^{-1}$) every step was maintained until stability was reached and then automatically changed to the next one. Temperature was set up at 22°C and fluctuated between 20.9 and

22.1°C and relative humidity fluctuated between 50 to 80% inside the measuring head. Controls were done as described on section 3.3.1. Results ranged from 0 to 0.5 $\mu\text{mol CO}_2 \text{ m}^{-2} \text{ s}^{-1}$ and were considered negligible.

3.3.3 Modelling

Light- and CO_2 -response curves were modelled and analyzed for several photosynthetic parameters. All the modelled data was calculated using net photosynthetic rates. Light response curves were modelled using Photosyn assistant software (Dundee scientific, University of Dundee, Dundee, UK) (Parsons et al. 1997). The software- does the modelling by a non-rectangular hyperbola in which the initial slope is the apparent quantum yield of CO_2 uptake ($\Phi_{\text{app CO}_2}$), the light compensation point and apparent respiration are estimated from axis intercepts and the light saturated maximum (A_{max}) is the upper asymptote. The software uses the equations of Prioul and Chartier (1977) to estimate the derived parameters. To calculate the modelled derived parameters from the CO_2 response curves the software uses the equations of Olsson and Leveranz (1994). CO_2 response curves are performed in a similar way as the light response curves except that the C_a is variable and irradiance remains constant at a saturated value. Carboxylation efficiency (CE) is defined as the slope of the initial curve and respiration is the Y-intercept of the line. CO_2 compensation point (Γ^*) is calculated as the X-intercept of the modelled curve.

3.4 Pigment Determination

3.4.1 Chlorophyll and Carotenoids

Chl *a*, *b* and total carotenoid content was determined spectrophotometrically from acetone extracts using a SmartSpec Plus spectrophotometer (Bio-Rad Laboratories, Hercules, CA, USA). Leaf material was weighed and ground in 1 mL of 80% (v/v) pre-chilled acetone (HPLC Grade; EMD Millipore, Darmstadt, Germany) using a pre-chilled mortar and a pestle containing sand (Standard Ottawa; EM Science, Merck KGaA, Darmstadt, Germany). The ground samples were transferred to 2 mL centrifuge tubes (USA Scientific, FL, USA) followed by centrifugation for 10 min at 13,200 rpm at 4°C (Microcentrifuge 5415R, Eppendorf AG, Hamburg, Germany). Supernatant from the

tubes was transferred to 15 mL tubes (VWR International; Radnor, PA, USA) volume was adjusted to 10 mL with 80%(v/v) acetone. Quantification of chlorophyll *a*, *b* and total carotenoids were calculated using the following equations: Chl *a* = $12.21A_{663} - 2.81A_{646}/229$; Chl *b* = $20.13A_{646} - 5.03A_{663}/229$; carotenoids = $1000A_{470} - 3.27C_a - 104C_b/229$ (Lichtenthaler and Wellburn 1983) and expressed on a fresh weight and area basis. The spectrophotometer was blanked with 80%(v/v) acetone using 0.7 mL quartz cuvettes and then absorbance was measured in 3 wavelengths 470, 646 and 667 as described by Lichtenthaler and Wellburn (1983). Leaf area measurement was calculated with a scaled picture with ImageJ freeware (National Institutes of Health, USA).

3.4.2 Anthocyanins

Anthocyanin contents were determined spectrophotometrically from methanolic extracts using a SmartSpec Plus spectrophotometer (Bio-Rad). Leaf samples were weighed and a scaled photograph was taken to calculate total area. Samples were placed in a 15 mL tube (VWR International) with 1 mL of 3 M HCl:H₂O:MeOH (1:3:16 by volume) respectively during 24 hours at 4°C in the dark with gentle agitation. After 24 hours all the content on the tubes was ground with a pre-chilled mortar and pestle with a small amount of sand (Standard Ottawa). Ground samples were transferred to 2 mL screw cap centrifuge tubes followed by centrifugation during 10 min at 13,200 rpm at 4°C (Microcentrifuge 5415R) supernatant was collected and volume adjusted. The spectrophotometer was blanked with acidified methanol. Using 1 mL plastic cuvettes absorbance was measured in two wavelengths 530 and 653. Anthocyanin levels were determined from the methanolic extract as $A_{530} - (0.24 * A_{653})$ (Gould et al. 2000) and expressed on a FW basis as *ABS*/FW and an area basis as *ABS*/area.

3.5 Photoinhibition of Photosynthesis

3.5.1 Photoinhibition

Detached leaves of Shandong and Yukon ecotypes of *Eutrema* of each growing condition LL and HL were assessed for photoinhibition of photosynthesis. Eight detached leaves of each ecotype of each condition were placed adaxial side up on a

petri dish with deionized water. Photoinhibition of photosynthesis was quantified by monitoring changes in F_v/F_m as a function to the exposure time to an irradiance of 1750 $\mu\text{mol photons m}^{-2} \text{ s}^{-1}$ (400W Bulb metal halide model E40 CLU1SL, Koninklijke Philips N.V., Amsterdam, Netherlands) during 2 hours in a cold room at 2°C under ambient air conditions. Irradiance was determined at the surface level of the samples using a light meter (LI-250; Li-Cor).

3.5.2 Chlorophyll Fluorescence

Chlorophyll *a* fluorescence was performed using a hand-held portable fluorometer (FP100, Photon System Instruments, Drasov, Czech Republic). Leaves were dark-adapted during 15 min at room temperature before the measurements.

Maximum photochemical quantum efficiency of PSII was calculated as $F_v/F_m = (F_m - F_o)/F_m$, where F_o and F_m represent the minimal and maximal fluorescence yield respectively for the dark-adapted states. For the photoinhibition experiment F_v/F_m as calculated at the beginning of the experiment and at the end of the exposure as described in section 3.5.1.

3.6 Statistics and Experimental Design

Descriptive statistics were used to describe data. The test samples were replicated at least 3 times for the different experiments. Average, standard deviation and standard error were calculated using Microsoft Excel (Microsoft Corporation, Redmond, WA, USA). Raw data was analyzed using either a one-way ANOVA or two-way ANOVA in Sigmaplot 12 (Systat Software Inc. San Jose, CA, USA). Data was tested for equal variance and a normality test (Shapiro-Wilk) performed. With the two-way ANOVA was possible to determine the difference among the ecotypes, difference among the growth irradiance levels and the interaction between ecotypes and growth irradiance. When a significant difference was observed a multiple comparison procedure was done using the Holm-Sidak method.

CHAPTER 4

4.0 Results

4.1 Growth Analyses

4.1.1 Absolute Growth Parameters

Phenological development of the Shandong and Yukon ecotypes of *Eutrema* under two different irradiance regimes is very similar and minimal differences in the measured parameters were found between the two ecotypes.

Development appeared to be faster under LL conditions for the Yukon ecotype (Fig. 4.1A). Results from FW and DW accumulation over time showed that by the end of the cycle there is a higher mass accumulation for plants grown under HL conditions (Fig. 4.1C and D and 4.2C and D).

Phenological development of the Shandong and Yukon ecotypes of *Eutrema* under LL and HL irradiance regimes was assessed as a function of time and several growth parameters calculated. There was a steady increase in FW for the entire time course irrespective of ecotype or growth irradiance (Fig. 4.1). Under LL conditions the Yukon ecotype demonstrated a greater FW accumulation in comparison to Shandong with the growth curves diverging after day 19 (Fig. 4.1A). In contrast, under HL conditions no differences were observed in FW between ecotypes (Fig. 4.1B). When the Shandong ecotype was examined under LL and HL regimes, greater FW accumulation was observed at HL (Fig. 4.1C). However, the Yukon ecotype demonstrated no differences between LL and HL conditions until day 27 where FW was greater for the HL grown plants (Fig. 4.1D). A similar trend for ecotypes and irradiance regimes was observed for DW accumulation (Fig. 4.2).

Upon examination of LA, the Yukon ecotype demonstrated much higher values under LL conditions in comparison to Shandong with the growth curves diverging after day 19 (Fig. 4.3A). A similar trend was observed between ecotypes under HL conditions although the differences were not as great (Fig. 4.3B). The irradiance regime had no effect on LA in either the Shandong or Yukon ecotype (Fig. 4.3C and D).

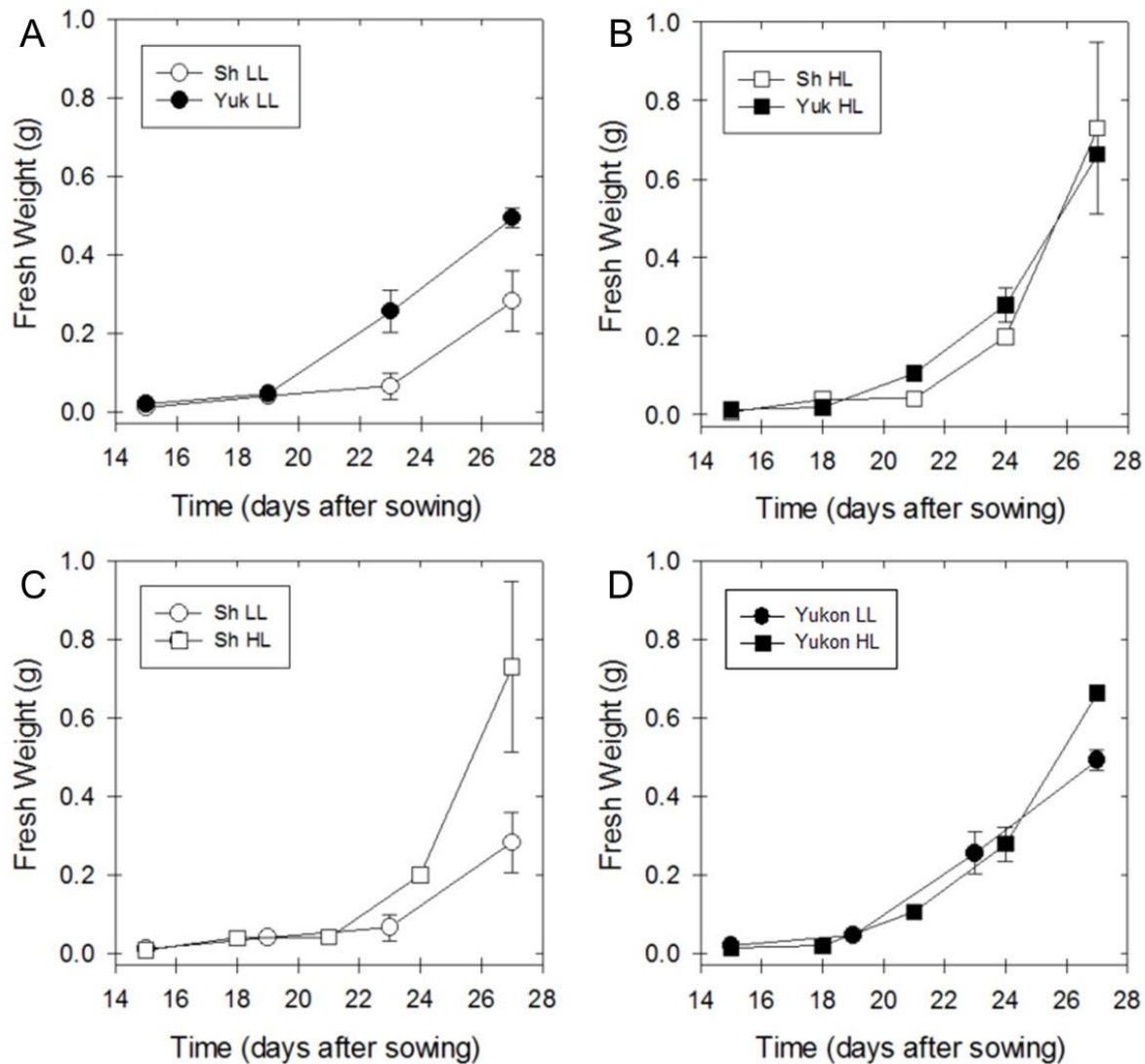


Figure 4.1 Fresh weight (FW) accumulation for the Shandong and Yukon ecotypes of *Eutrema* developed at different growth irradiances. Plants of each ecotype were grown under either 250 (LL) or 750 $\mu\text{mol photons m}^{-2} \text{s}^{-1}$ (HL) PPFD. FW was calculated as the total aerial portion of the plant. Shandong LL (○); Yukon LL (●); Shandong HL (□); Yukon HL (■). Ecotypic comparison under LL (A) and HL (B) conditions. Growth irradiance comparisons for the Shandong (C) and Yukon (D) ecotypes. Values represent means \pm SD ($n = 3$ to 5). FW, fresh weight; HL, high-light; LL, low-light; PPFD, photosynthetic photon flux density; SD, standard deviation.

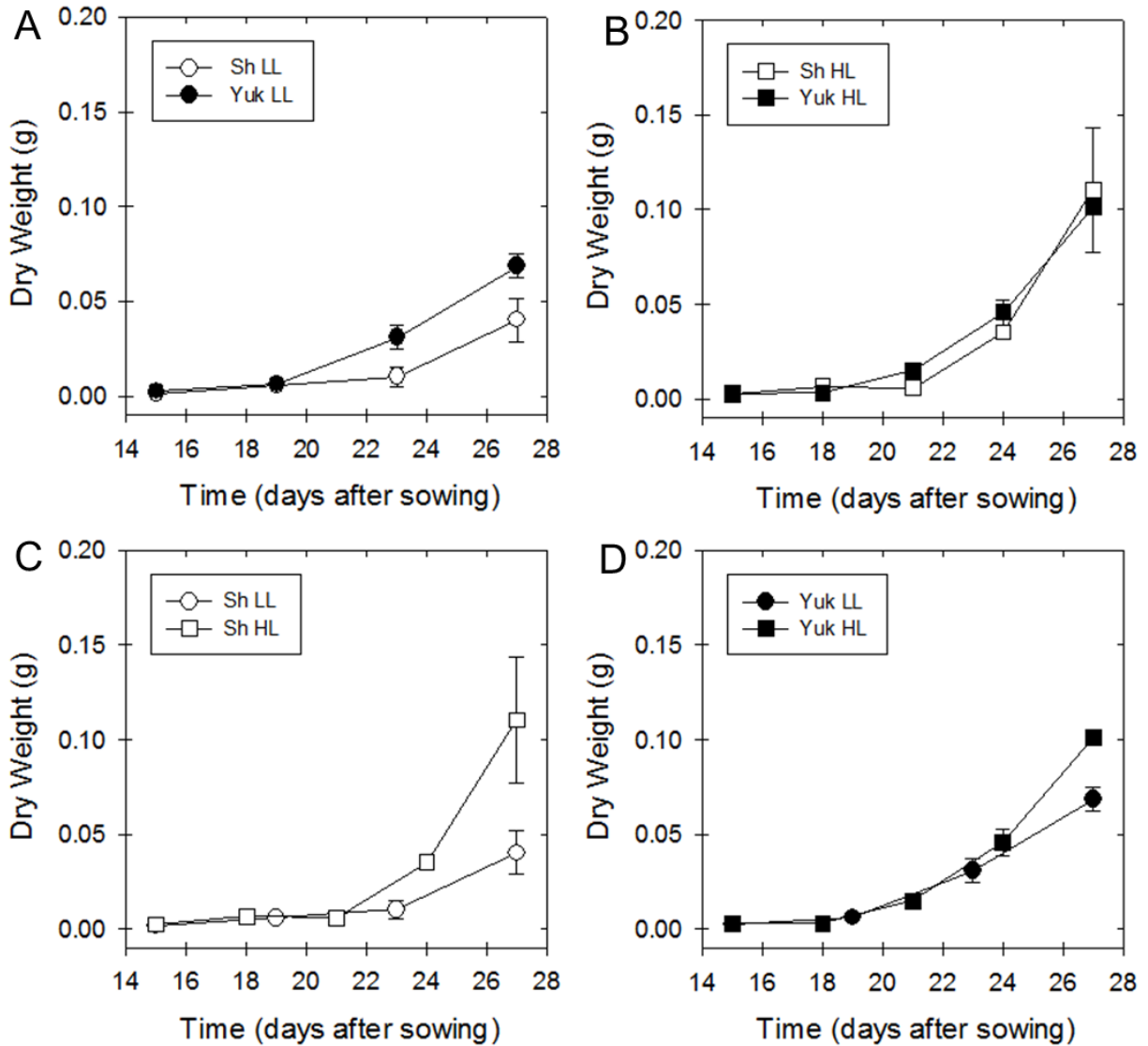


Figure 4.2 Dry weight (DW) accumulation for the Shandong and Yukon ecotypes of *Eutrema* developed at different growth irradiance. Plants of each ecotype were grown under either 250 (LL) or 750 $\mu\text{mol photons m}^{-2} \text{s}^{-1}$ (HL) PPFD. DW was calculated as the total aerial portion of the plant. Shandong LL (○); Yukon LL (●); Shandong HL (□); Yukon HL (■). Ecotypic comparison under LL (A) and HL (B) conditions. Growth irradiance comparisons for the Shandong (C) and Yukon (D) ecotypes. Values represent means \pm SD ($n = 3$ to 5). DW, dry weight; HL, high-light; LL, low-light; PPFD, photosynthetic photon flux density; SD, standard deviation.

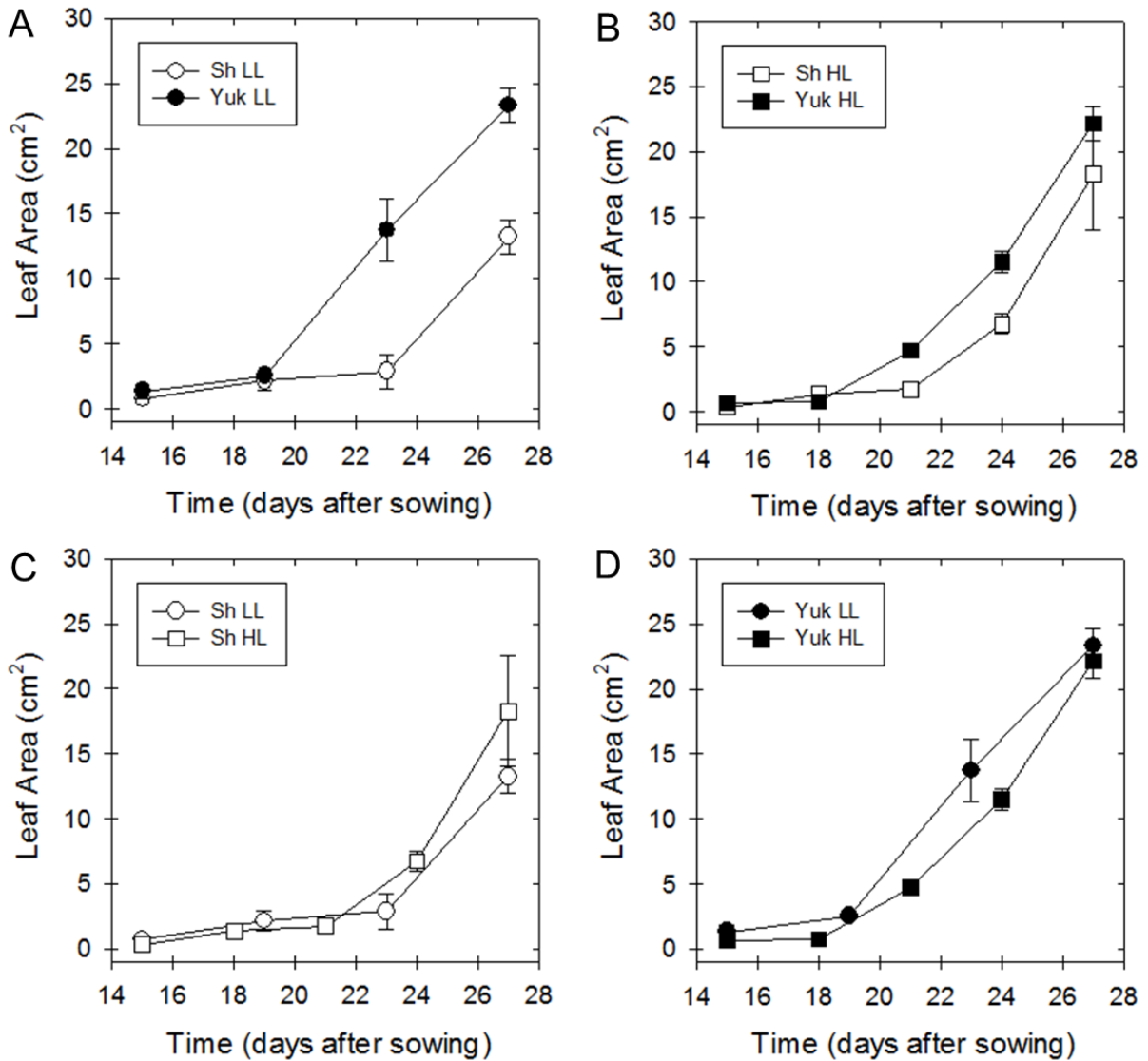


Figure 4.3 Total leaf area (LA) for the Shandong and Yukon ecotypes of *Eutrema* developed at different growth irradiances. Plants of each ecotype were grown under either 250 (LL) or 750 $\mu\text{mol photons m}^{-2} \text{s}^{-1}$ (HL) PPFD. Shandong LL (○); Yukon LL (●); Shandong HL (□); Yukon HL (■). Ecotypic comparison under LL (A) and HL (B) conditions. Growth irradiance comparisons for the Shandong (C) and Yukon (D) ecotypes. Values represent means \pm SD ($n = 3$ to 5). HL, high-light; LA, leaf area; LL, low-light; PPFD, photosynthetic photon flux density; SD, standard deviation.

Under growth conditions of LL the Shandong and Yukon ecotypes presented similar leaf number in the initial developmental stages with Yukon producing more leaves than Shandong at the later stages (Fig. 4.4A). Growth under HL conditions resulted in similar leaf numbers for both ecotypes (Fig. 4.4B). The irradiance regime had no effect on leaf number in either the Shandong or Yukon ecotype (Fig. 4.4C and D).

4.1.2 Relative Growth Parameters

Leaf water content remained relatively constant for the duration of the time course with essentially no differences between ecotypes or growth irradiance (Fig. 4.5). The Shandong ecotype exhibited a lower water content than that of Yukon under HL conditions for the initial sampling point (Fig. 4.5B). The water contents for all plants under HL conditions were lower compared to LL plants for the first sampling point (Fig. 4.5C and D). This might be due to the high irradiance and heat emitted from the light source that probably affected the water contents on the first stages of development when these plants were small.

Fresh weight to dry weight ratio shows slightly lower values for the Shandong ecotype under LL conditions (Fig. 4.6A) Under HL conditions FW:DW ratio is very similar and minimal differences were found between the two ecotypes (Fig. 4.6C and D). Fresh to dry weight ratio under LL conditions for both ecotypes exhibit a different trend. Shandong has lower values over the examined time course. For day 19 there is a closer ratio and the last point does not show difference between the two ecotypes (Fig. 4.6A). Fresh to dry weight ratio under HL conditions is very similar between Shandong and Yukon ecotypes. For the first point Shandong has a lower starting point and after the second measuring point (Day 19) both ecotypes show very close FW:DW (Fig. 4.6B). Fresh to dry weight ratio for the Shandong ecotype under LL and HL conditions exhibit a different behavior between the two growth irradiances. The plants grown under LL conditions have a relatively constant ratio while HL plants have a more variable pattern of FW:DW. HL plants start with a low ratio that increases until day 21 and then a small decrease to end up with a value close to the peak of day 21 (Fig. 4.6C). Fresh to dry weight ratio on the Yukon ecotype grown under LL and HL conditions have a similar trend as the one observed for the Shandong ecotype when a comparison was made. LL

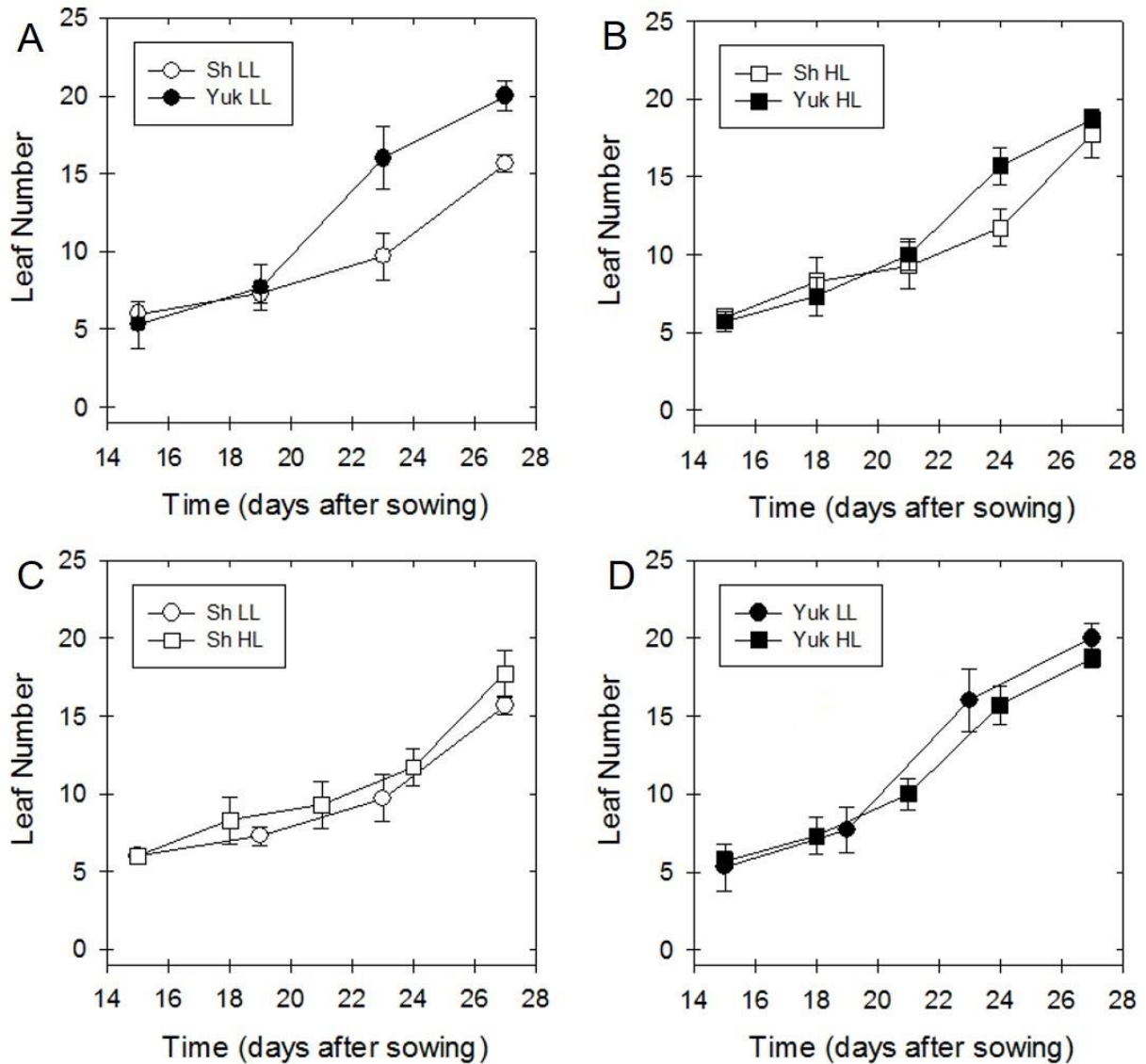


Figure 4.4 Number of accumulated leaves for the Shandong and Yukon ecotypes of *Eutrema* developed at different growth irradiances. Plants of each ecotype were grown under either 250 (LL) or 750 $\mu\text{mol photons m}^{-2} \text{s}^{-1}$ (HL) PPFD. Shandong LL (○); Yukon LL (●); Shandong HL (□); Yukon HL (■). Ecotypic comparison under LL (A) and HL (B) conditions. Growth irradiance comparisons for the Shandong (C) and Yukon (D) ecotypes. Values represent means \pm SD ($n = 3$ to 5). HL, high-light; LL, low-light; PPFD, photosynthetic photon flux density; SD, standard deviation.

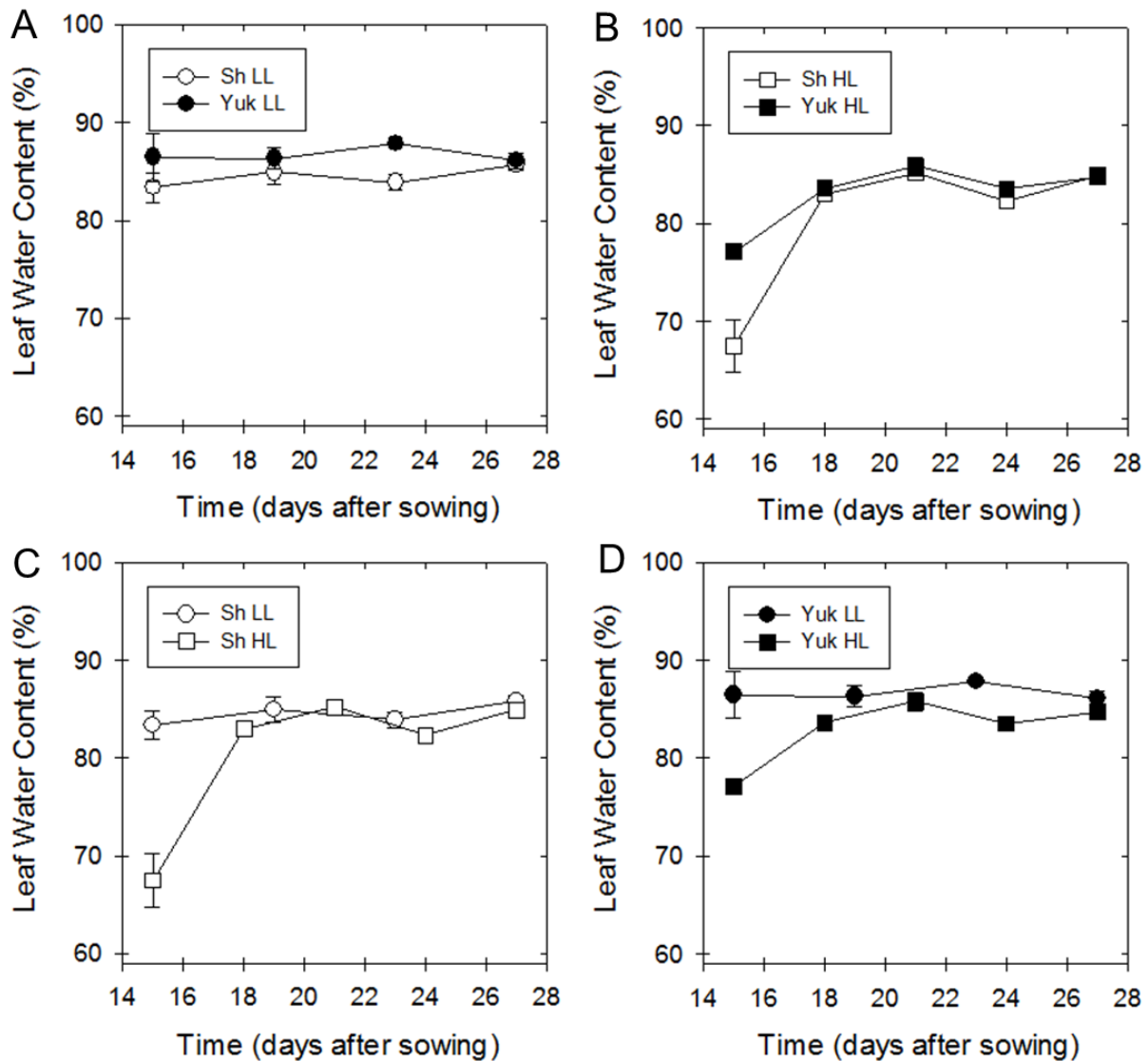


Figure 4.5 Leaf water content for the Shandong and Yukon ecotypes of *Eutrema* developed at different growth irradiances. Plants of each ecotype were grown under either 250 (LL) or 750 $\mu\text{mol photons m}^{-2} \text{s}^{-1}$ (HL) PPFD. Leaf relative water content was estimated as $((\text{FW}-\text{DW})/\text{FW}) \times 100$. Shandong LL (○); Yukon LL (●); Shandong HL (□); Yukon HL (■). Ecotypic comparison under LL (A) and HL (B) conditions. Growth irradiance comparisons for the Shandong (C) and Yukon (D) ecotypes. Values represent means \pm SD ($n = 3$ to 5). DW, dry weight; FW, fresh weight; HL, high-light; LL, low-light; PPFD, photosynthetic photon flux density.

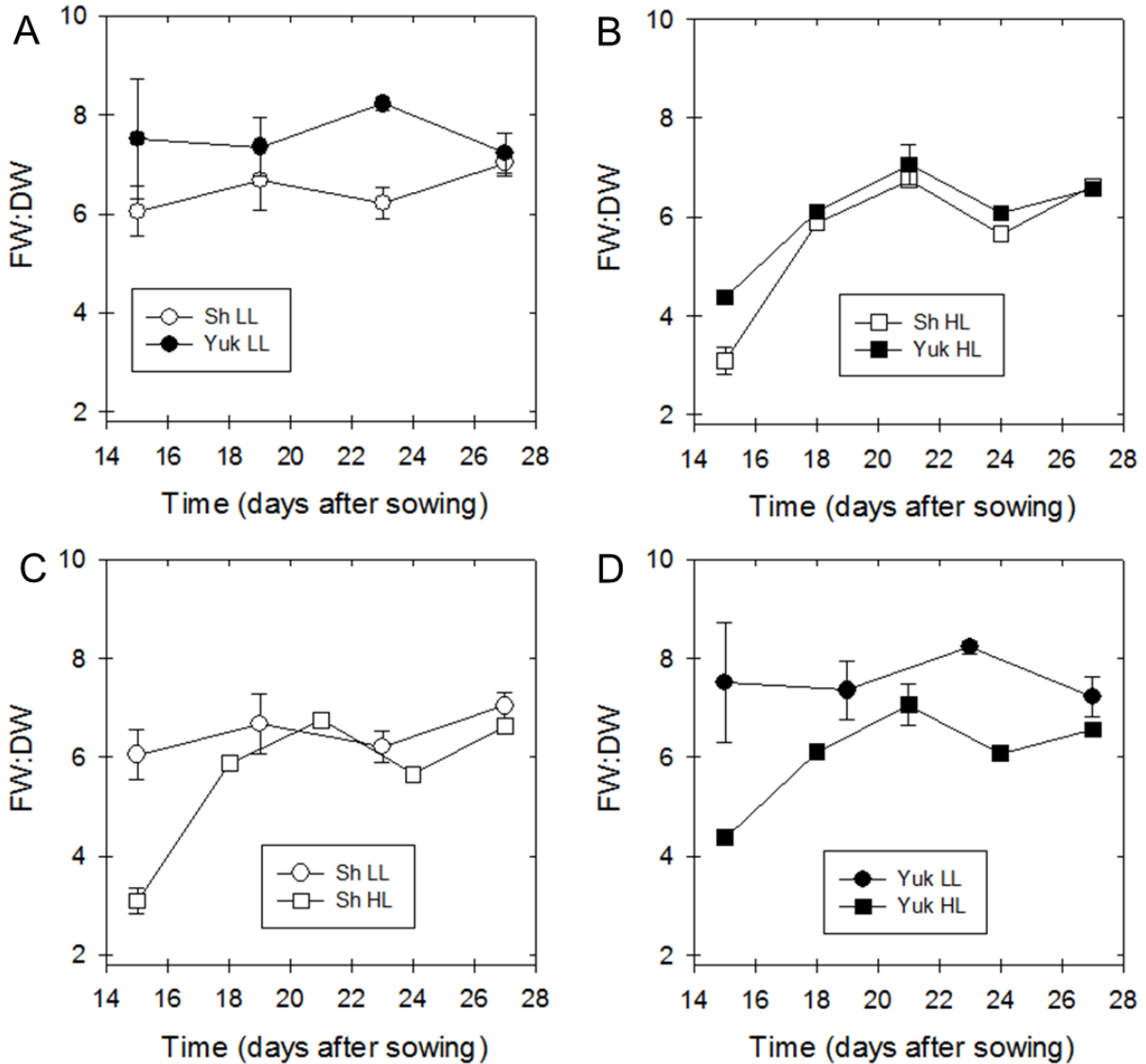


Figure 4.6 Fresh weight to dry weight ratio (FW:DW) for the Shandong and Yukon ecotypes of *Eutrema* developed at different growth irradiances. Plants of each ecotype were grown under either 250 (LL) or 750 $\mu\text{mol photons m}^{-2}\text{s}^{-1}$ (HL) PPFD. Shandong LL (○); Yukon LL (●); Shandong HL (□); Yukon HL (■). Ecotypic comparison under LL (A) and HL (B) conditions. Growth irradiance comparisons for the Shandong (C) and Yukon (D) ecotypes. Values represent means \pm SD ($n = 3$ to 5). DW, dry weight; FW, fresh weight; HL, high-light; LL, low-light; PPFD, photosynthetic photon flux density; SD, standard deviation.

plants have a higher FW to DW ratio and it remains relatively constant through all the measured points. Yukon plants grown under HL conditions had more variable FW to DW ratios with a low starting point and then an increase until day 21 and then a decrease and a final point slightly lower than the highest peak by day 21 (Fig. 4.6D). Fresh weight to dry weight ratios remain relatively constant for plants grown under LL conditions irrespective of the ecotype while plants that were grown under HL conditions exhibited a more variable pattern through the sampling points this might be due to the different photoacclimation mechanisms that the plants have to cope with the increased light levels and to the heat generated by the lights as well.

SLA for the Shandong ecotype grown under LL and HL conditions shows a different trend. Under LL conditions there is a steady increase up to day 23 and then it decreases sharply. Under HL conditions initially SLA is higher than plants under LL conditions, then there is a decrease and an increase towards the last point (Fig. 4.7C). SLA for the Yukon ecotype grown under LL and HL conditions has a different trend. Under LL conditions SLA starts at a higher point than under HL conditions and it has a variable pattern, decreasing initially then a slight increase followed by a decrease until the last point For HL conditions the SLA has a steady increase until day 23 and then decreases constantly until the last point (Fig. 4.7D). Regardless of the growth irradiance were plants were grown Shandong always exhibits lower SLA values compared to Yukon based on these results Yukon appears to have thicker leaves than Shandong. Another observed characteristic is that an increase in the growth irradiance levels also leads to lower SLA levels. Under LL conditions for both ecotypes the starting point is the highest peak and there is a decrease towards the end with some variations between both ecotypes. For both ecotypes grown under HL conditions there is a similar trend with low values in both ends and a peak in the middle. Relative growth rates (RGR) were calculated on a DW basis over a 12 day growth interval for both ecotypes under LL and HL conditions and are presented in Table 4.1. There is no significant difference between the Shandong and Yukon ecotypes. Under either LL ($P = 0.901$) or HL ($P = 0.247$) conditions. The RGR for the Shandong ecotype was greater under HL condition ($P = 0.030$) in comparison to LL conditions while the Yukon ecotype showed no

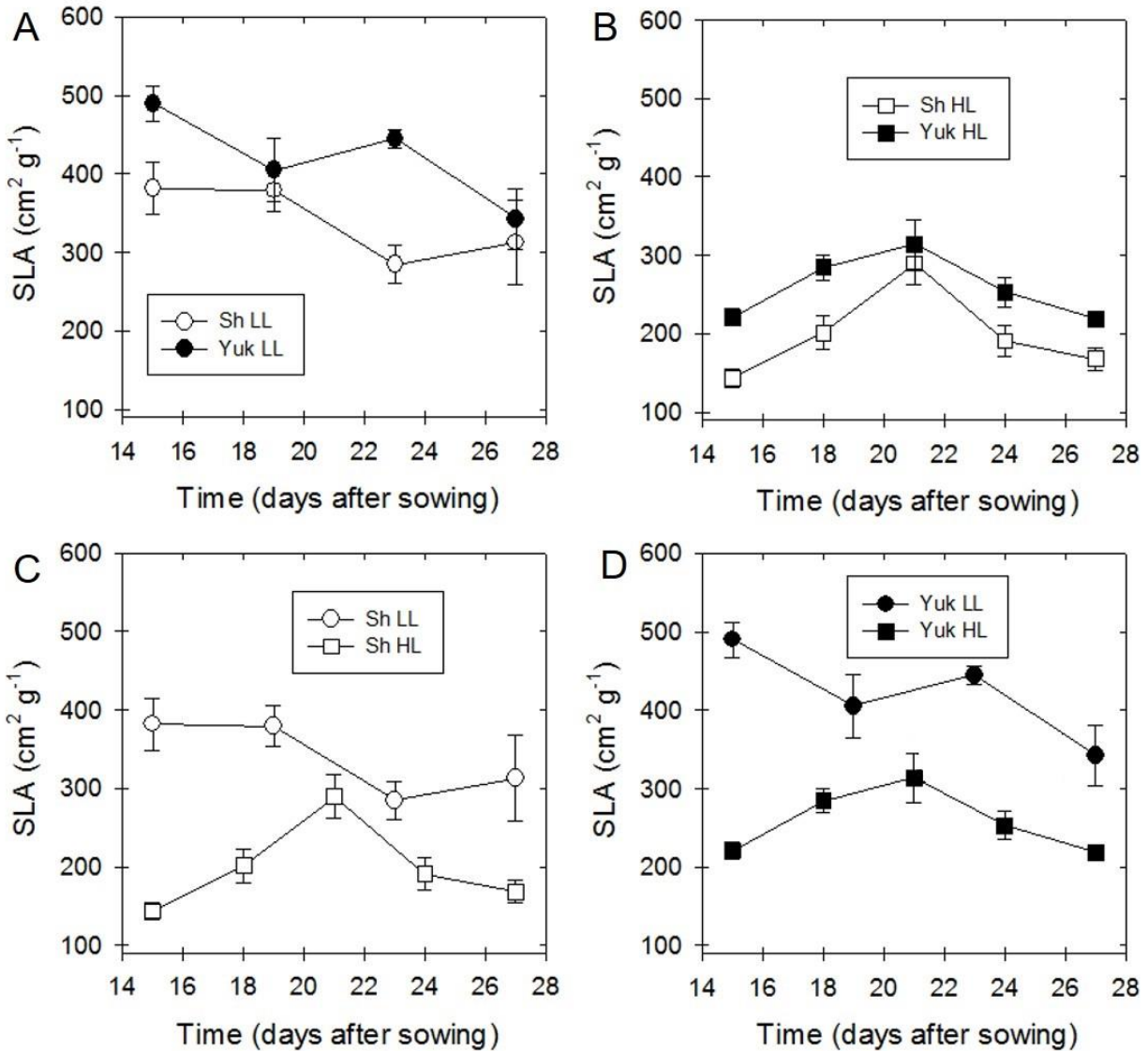


Figure 4.7 Specific leaf area (SLA) for the Shandong and Yukon ecotypes of *Eutrema* developed at different growth irradiances. Plants of each ecotype were grown under either 250 (LL) or 750 $\mu\text{mol photons m}^{-2} \text{s}^{-1}$ (HL) PPFD. Specific leaf area was calculated based on DW. Shandong LL (○); Yukon LL (●); Shandong HL (□); Yukon HL (■). Ecotypic comparison under LL (A) and HL (B) conditions. Growth irradiance comparisons for the Shandong (C) and Yukon (D) ecotypes. Values represent means \pm SD ($n = 3$ to 5). DW, dry weight; HL, high-light; LL, low-light; PPFD, photosynthetic photon flux density; SD, standard deviation; SLA, specific leaf area.

difference ($P = 0.377$) in response to growth irradiance. No statistically significant interaction was found between ecotype and growth irradiance ($P = 0.340$).

Representative photographs of the Shandong and Yukon ecotypes of *Eutrema* under LL and HL conditions are shown in Fig. 4.8. Both ecotypes display typical rosettes and at the stages indicated are all relatively comparable based on growth kinetics analyses (Figs. 4.1 to 4.7). One of the main characteristics to differentiate Shandong from Yukon is the serrated leaf margin (Fig. 4.8A and C). Under HL conditions the Shandong ecotype has petioles that are shorter than in the plants grown under LL (Figs. 4.8A and C). Upon visual observation leaves display a purple colour in the abaxial side. The Yukon ecotype under HL conditions looks very similar to the plants grown under LL conditions (Fig. 4.8B and D). However, the leaves are thicker and darker green than those grown under LL conditions according to visual observation of the plants.

Table 4.1 Relative growth rates (RGR) for the Shandong and Yukon ecotypes of *Eutrema* developed at different growth irradiance. Plants of each ecotype were grown under either 250 (LL) or 750 $\mu\text{mol photons m}^{-2} \text{s}^{-1}$ (HL) PPFD. RGR was calculated on a DW basis over a growth interval from 15 to 27 days after sowing. The data was analyzed using a two-way ANOVA and a multiple comparison test was done using the Holm-Sidak method. Different letters indicate a significant difference at $P = 0.05$. Values represent means \pm SD ($n = 3$ to 5). ANOVA, analysis of variance; DW, dry weight; HL, high-light; LL, low-light; PPFD, photosynthetic photon flux density; RGR, relative growth rate; SD, standard deviation.

Ecotype	RGR ($\text{g g}^{-1} \text{day}^{-1}$)	
	LL	HL
Shandong	0.272 ± 0.0187^b	0.317 ± 0.0307^a
Yukon	0.274 ± 0.0361^b	0.292 ± 0.00132^{ab}

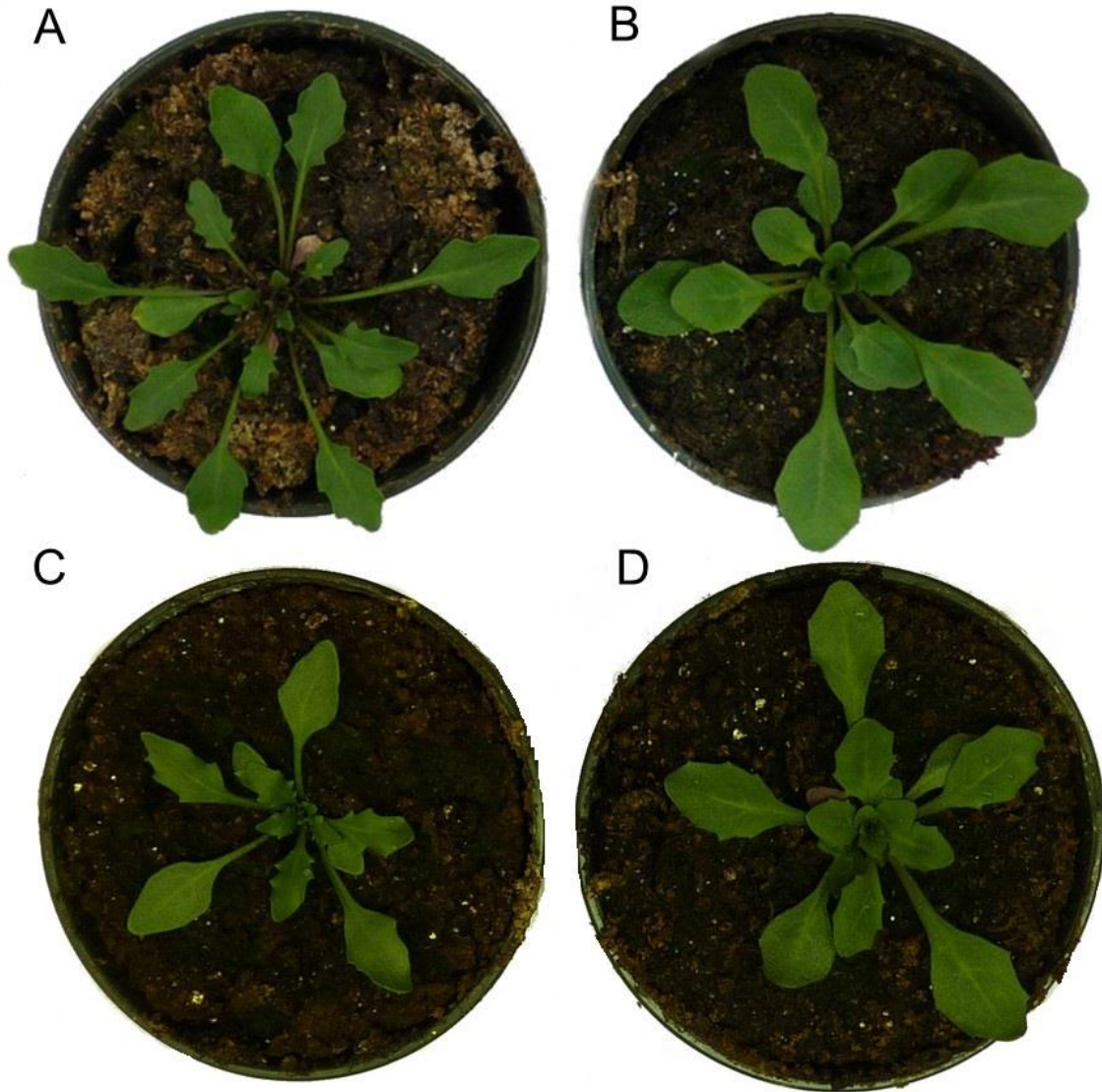


Figure 4.8 Phenotypic comparisons for the Shandong (**A, C**) and Yukon (**B, D**) ecotypes of *Eutrema* developed at different growth irradiance. Plants of each ecotype were grown under either 250 (LL; **A, B**) or 750 $\mu\text{mol photons m}^{-2} \text{s}^{-1}$ (HL; **C, D**) PPFD. Plants were photographed at 24 d for LL and 22 d for HL conditions for both ecotypes. Representative images are shown. HL, high-light; LL, low-light; PPFD, photosynthetic photon flux density.

4.2 Pigments

4.2.1 Chlorophyll and Carotenoids

Total chlorophyll estimated in a FW basis shows that there is no difference within plants grown under LL conditions ($P = 0.737$) same observation was found within plant grown under HL conditions ($P = 0.124$). When a comparison was made within ecotypes under LL and HL conditions a statistically significant difference was found for the two ecotypes ($P \leq 0.001$). No significant interaction was found between ecotype and growth irradiance ($P = 0.171$). Total chlorophyll estimated on an area basis showed a statistically significant difference within plants grown under LL ($P = 0.003$) and HL conditions ($P \leq 0.001$). The Shandong ecotype exhibits a difference when grown under different light regimes ($P \leq 0.001$) showing an increase in total chlorophyll contents on an area basis. Conversely the Yukon ecotype does not shows a difference in total chlorophyll between the two regimes on an area basis ($P = 0.226$). No significant interaction was found between ecotype and growth irradiance ($P = 0.122$). (Table 4.2).

Total carotenoids estimated on a FW basis shows no difference between ecotypes irrespective of the growth irradiance. No statistically significant interaction either was found between ecotype and growth irradiance ($P = 0.557$). Total carotenoids estimated on an area basis showed a significant difference between the two ecotypes under LL and HL conditions ($P = 0.004$ and $P \leq 0.001$). A difference within the Shandong ecotype show that there is a change when this plants are grown under contrasting light conditions ($P \leq 0.001$). Same results were obtained within the Yukon ecotype ($P = 0.002$). (Table 4.2). No statistically significant interaction was found between ecotype and growth irradiance ($P = 0.087$).

Chl *a:b* ratio are similar for the two ecotypes under LL conditions and no difference was found ($P = 0.649$). Under HL conditions the Yukon ecotype increases the *a:b* ratio but the Shandong remains with very similar values as in LL conditions a statistically significant difference was found ($P = 0.034$) (Table 4.2). No statistically significant interaction between ecotype and growth irradiance was found ($P = 0.060$).

Chl to Car ratio shows no difference between the Shandong and Yukon ecotype under LL conditions ($P = 0.940$) and under HL conditions ($P = 0.170$). However, when an ecotypic comparison was made the Shandong ecotype displayed significant

differences between the two growth conditions ($P \leq 0.001$). Same results were observed for the Yukon ecotype and a difference was found between the two light conditions ($P \leq 0.001$). (Table 4.2). No statistically significant interaction was found between ecotype and growth irradiance ($P = 0.283$).

Table 4.2 Leaf chlorophyll and carotenoid contents for the Shandong and Yukon ecotypes of *Eutrema* developed at different growth irradiance. Plants of each ecotype were grown under either 250 (LL) or 750 $\mu\text{mol photons m}^{-2} \text{s}^{-1}$ (HL) PPFD. The data were analyzed using a two-way ANOVA and a multiple comparison test was done using the Holm-Sidak method. Different letters indicate a significant difference at $P = 0.05$. Values represent means \pm SD ($n = 7$). ANOVA, analysis of variance; c, carotenes; Car, carotenoid; Chl, chlorophyll; FW, fresh weight; HL, high-light; LL, low-light; PPFD, photosynthetic photon flux density; SD, standard deviation; x, xanthophylls.

Ecotype and growth irradiance	Total Chl (a+b)	Total Car (c+x)	Total Chl (a+b)	Total Car (c+x)	Chl a:b	Chl:Car
	$\mu\text{g g FW}^{-1}$		$\mu\text{g cm}^{-2}$			
Shandong LL	1092.79 \pm 178.79 ^a	195.22 \pm 35.32 ^a	32.17 \pm 6.86 ^b	5.72 \pm 1.11 ^c	4.42 \pm 0.26 ^b	5.62 \pm 0.39 ^a
Yukon LL	1110.14 \pm 129.98 ^a	197.40 \pm 18.17 ^a	24.45 \pm 3.10 ^c	4.38 \pm 0.74 ^d	4.30 \pm 0.62 ^b	5.64 \pm 0.58 ^a
Shandong HL	911.59 \pm 140.67 ^b	187.75 \pm 28.56 ^a	41.48 \pm 9.42 ^a	8.56 \pm 1.95 ^a	4.77 \pm 0.77 ^b	4.88 \pm 0.58 ^b
Yukon HL	822.09 \pm 76.51 ^b	181.24 \pm 16.70 ^a	27.93 \pm 6.38 ^c	6.05 \pm 0.72 ^b	5.40 \pm 1.22 ^a	4.58 \pm 0.68 ^b

4.2.2 Anthocyanin

Total anthocyanin contents on a FW basis does not exhibit statistically significant differences for plants grown under LL conditions ($P = 0.053$). However, the other comparisons made showed statistically significant differences. Plants of both ecotypes grown under HL conditions showed a significant difference ($P = <0.001$). Ecotypic comparisons showed differences within the Shandong ecotype ($P = <0.001$) this ecotype exhibited a decrease in anthocyanin levels on a FW basis. The Yukon ecotype under the two growth conditions showed a statistically significant difference ($P = 0.036$). However, a contrasting result was observed when compared to Shandong, Yukon increased the anthocyanin levels as a response to a higher growth irradiance. A statistically significant interaction was found between ecotype and growth irradiance ($P < 0.001$). Total anthocyanin contents on an area basis shows no difference between the Shandong and Yukon ecotypes under LL conditions ($P = 0.168$). Under HL conditions there is a statistically significant difference ($P = 0.001$). When a comparison was made within the Shandong ecotype under LL and HL conditions a statistically significant difference was observed ($P = 0.005$) and same results were observed for the Yukon ecotype showing a difference in anthocyanin levels between the two growth conditions ($P = 0.044$) (Table 4.3). A statistically significant interaction was found between ecotype and growth irradiance ($P = 0.002$).

Table 4.3 Leaf anthocyanin content for the Shandong and Yukon ecotypes of *Eutrema* developed at different growth irradiance. Plants of each ecotype were grown under either 250 (LL) or 750 $\mu\text{mol photons m}^{-2} \text{s}^{-1}$ (HL) PPFD. The data was analyzed using a two-way ANOVA and a multiple comparison test was done using the Holm-Sidak method. Different letters within columns indicate a significant difference at $P = 0.05$. Values represent means \pm SD ($n = 3$). ANOVA, analysis of variance; FW, fresh weight; HL, high-light; LL, low-light; PPFD, photosynthetic photon flux density; SD, standard deviation.

Ecotype	Growth Irradiance	Total Anthocyanin	Total Anthocyanin
		$A_{530} \text{ g FW}^{-1}$	$A_{530} \text{ cm}^{-2}$
Shandong	LL	12.35 ± 1.14^{ab}	0.26 ± 0.08^b
Yukon	LL	9.60 ± 0.58^b	0.18 ± 0.02^b
Shandong	HL	1.08 ± 0.27^c	0.05 ± 0.01^c
Yukon	HL	12.64 ± 2.67^a	0.31 ± 0.11^a

4.3 Photosynthesis

4.3.1 Light Responses

Photosynthetic light response curves were done for each growing condition (LL and HL) for both the Shandong and Yukon ecotypes of *Eutrema*. The measurements were done as described in section 3.3.1.

The light response curve for the Shandong and Yukon ecotypes grown under LL conditions done with at 200 C_a shows a similar trend. The Yukon ecotype exhibits a higher dark respiration rate than Shandong (Fig. 4.9A). Under similar conditions the light response curve of plants grown under HL conditions show that the Shandong ecotype has higher rates of dark respiration and higher photosynthetic rates when compared to the Yukon ecotype grown under similar conditions (Fig. 4.9B).

A comparison of the Shandong ecotype grown under LL and HL conditions shows that the plants grown under LL regimes exhibit lower dark respiration rates and lower photosynthetic rates through the final steps of the light response curve when compared to the plants grown under HL conditions (Fig. 4.9C).

The light response curve for the Yukon ecotype under LL and HL conditions showed a similar trend with minimal differences like a lower dark respiration rate for plants grown under LL conditions and a slight tendency to have higher photosynthetic rates as well (Fig. 4.9D).

For the light response curves done with an ambient level of 400 C_a the Shandong and Yukon ecotypes grown under LL conditions show the same trend and no differences between the responses are appreciated (Fig. 4.10A). Under the same ambient conditions the Shandong and Yukon ecotypes grown under HL conditions exhibit some differences in the responses. The Shandong ecotype has higher dark respiration rates and higher net photosynthetic rates than the Yukon ecotype (Fig. 4.10B). The light response curve for the Yukon ecotype under LL and HL conditions show a similar trend with minimal differences like a lower dark respiration rate for plants grown under LL conditions and a slight tendency to have higher photosynthetic rates as well (Fig. 4.10D).

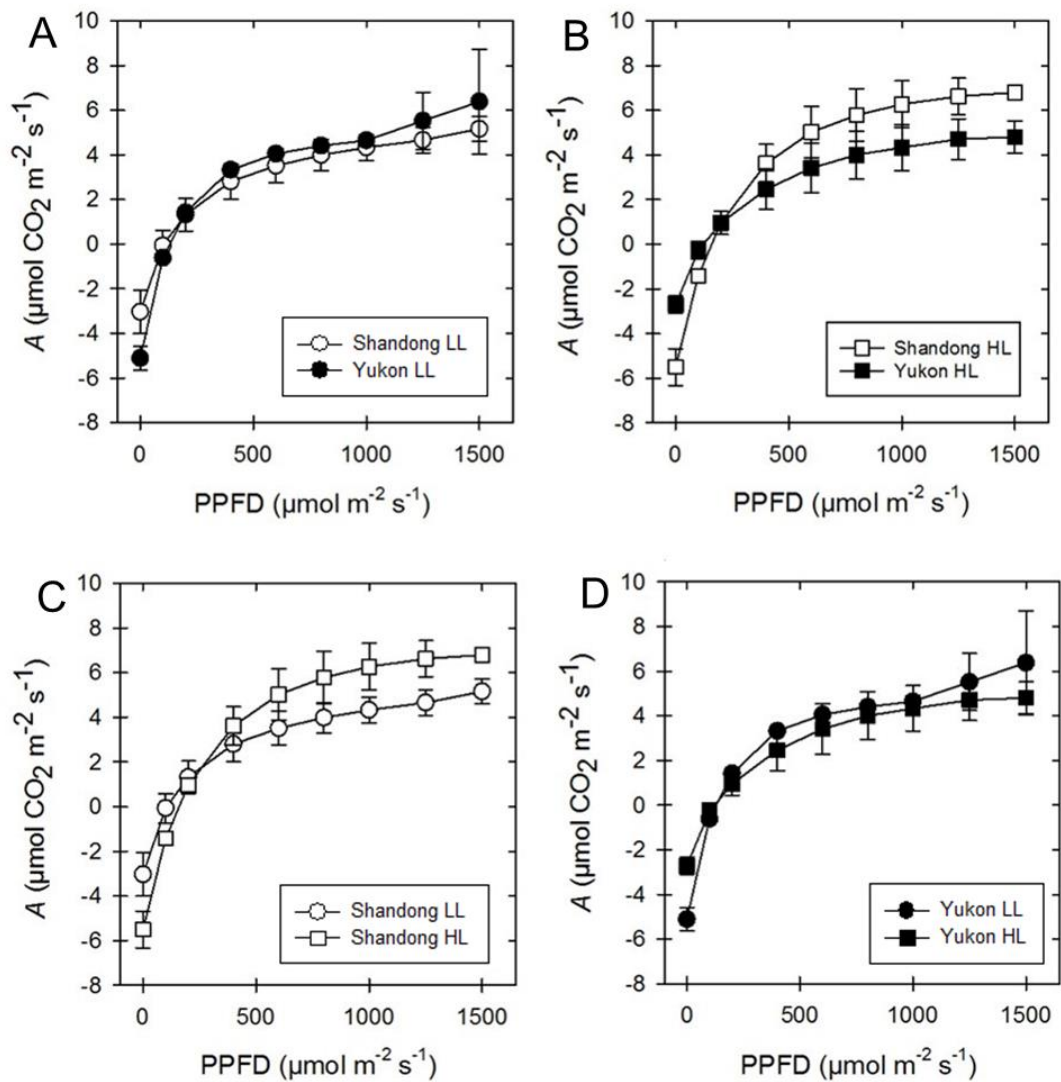


Figure 4.9 Light-response curves at 200 C_a for the Shandong and Yukon ecotypes of *Eutrema* developed at different growth irradiance. Plants of each ecotype were grown under either 250 (LL) or 750 $\mu\text{mol photons m}^{-2} \text{s}^{-1}$ (HL) PPFD. Light was set up in 9 steps (1500, 1250, 1000, 800, 600, 400, 200, 100, 0 $\mu\text{mol photons m}^{-2} \text{s}^{-1}$), leaf temperature was maintained at 22°C and relative humidity 50-80%. Shandong LL (○); Yukon LL (●); Shandong HL (□); Yukon HL (■). Ecotypic comparison under LL (A) and HL (B) conditions. Growth irradiance comparisons for the Shandong (C) and Yukon (D) ecotypes. Values represent means \pm SE ($n = 6$ to 9). HL, high-light; LL, low-light; PPFD, photosynthetic photon flux density; SE, Standard error.

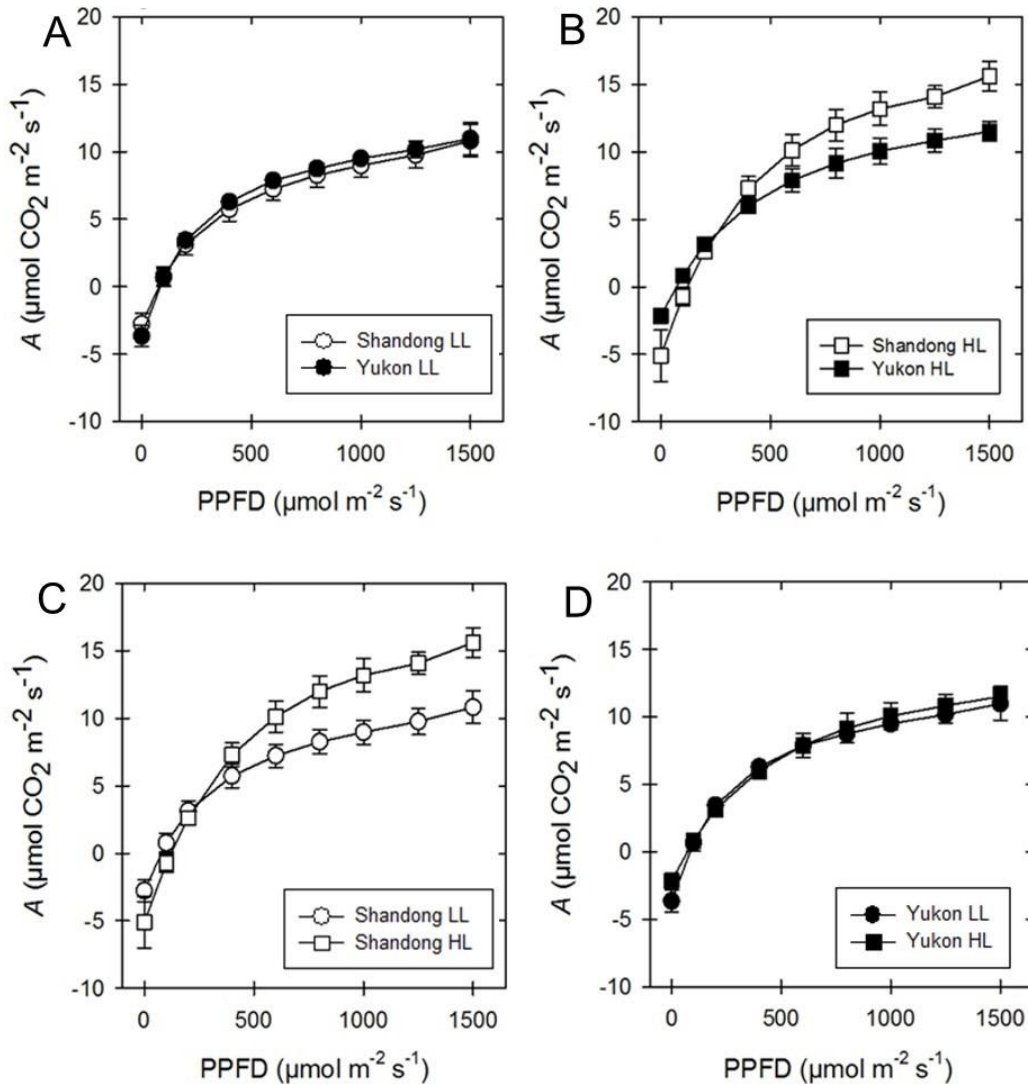


Figure 4.10 Light-response curves at 400 C_a for the Shandong and Yukon ecotypes of *Eutrema* developed at different growth irradiance. Plants of each ecotype were grown under either 250 (LL) or 750 $\mu\text{mol photons m}^{-2} \text{ s}^{-1}$ (HL) PPFD. Light was set up in 9 steps (1500, 1250, 1000, 800, 600, 400, 200, 100, 0 $\mu\text{mol photons m}^{-2} \text{ s}^{-1}$), leaf temperature was maintained at 22°C and relative humidity 50-80%. Shandong LL (○); Yukon LL (●); Shandong HL (□); Yukon HL (■). Ecotypic comparison under LL (A) and HL (B) conditions. Growth irradiance comparisons for the Shandong (C) and Yukon (D) ecotypes. Values represent means \pm SE ($n = 6$ to 11). HL, high-light; LL, low-light; PPFD, photosynthetic photon flux density; SE, Standard error.

The response of the Shandong ecotype under LL and HL conditions shows that plants grown under HL conditions have higher dark respiration rates and higher photosynthetic rates than the plants grown under LL conditions (Fig. 4.10C). When a comparison was done between the Yukon ecotype grown under LL and HL conditions the differences in the light response curve between the two growing conditions are negligible (Fig. 4.10D).

The light response curves done with an ambient concentration of 800 C_a exhibit minimal differences for the under LL conditions for the Shandong and Yukon ecotypes. (Fig. 4.11A). The same situation was observed for the Yukon ecotype grown under LL and HL conditions were minimal differences in net photosynthetic rates were observed. The most notable result for these light response curves was the Shandong ecotype under HL conditions. This ecotype had a higher response to saturated concentrations of CO_2 exhibiting higher net photosynthetic rates when compared to the other plants particularly after the irradiance of the light curve exceeded 400 $\mu\text{mol photons m}^{-2} \text{s}^{-1}$ (Fig. 4.11B and C).

4.3.1.1 Photosynthetic Derived Parameters at 200 C_a

Calculated photosynthetic parameters from the modelled data showed that the A_{max} does not exhibit a difference for the two ecotypes when grown under LL conditions ($P = 0.295$). No difference was found either for the Yukon ecotype when the two growth regimes were compared ($P = 0.064$) indicating that there is no change for this ecotype when is grown under increased irradiance. In contrast the Shandong ecotype increases A_{max} when grown under to the HL regime, there is a difference respect Shandong plants grown under LL conditions ($P = 0.006$) and also when compared to the Yukon ecotype under HL conditions ($P = <0.001$) (Table 4.4). A statistically significant interaction was found between ecotype and growth irradiance ($P = 0.002$).

The calculated $\Phi_{\text{app}} CO_2$ shows no difference for the two ecotypes grown under LL conditions ($P = 0.094$). No difference was found for the Shandong ecotype between the two growth conditions ($P = 0.843$). Interestingly, the Yukon ecotype decreases the $\Phi_{\text{app}} CO_2$ when grown under HL conditions and there is a difference when is grown

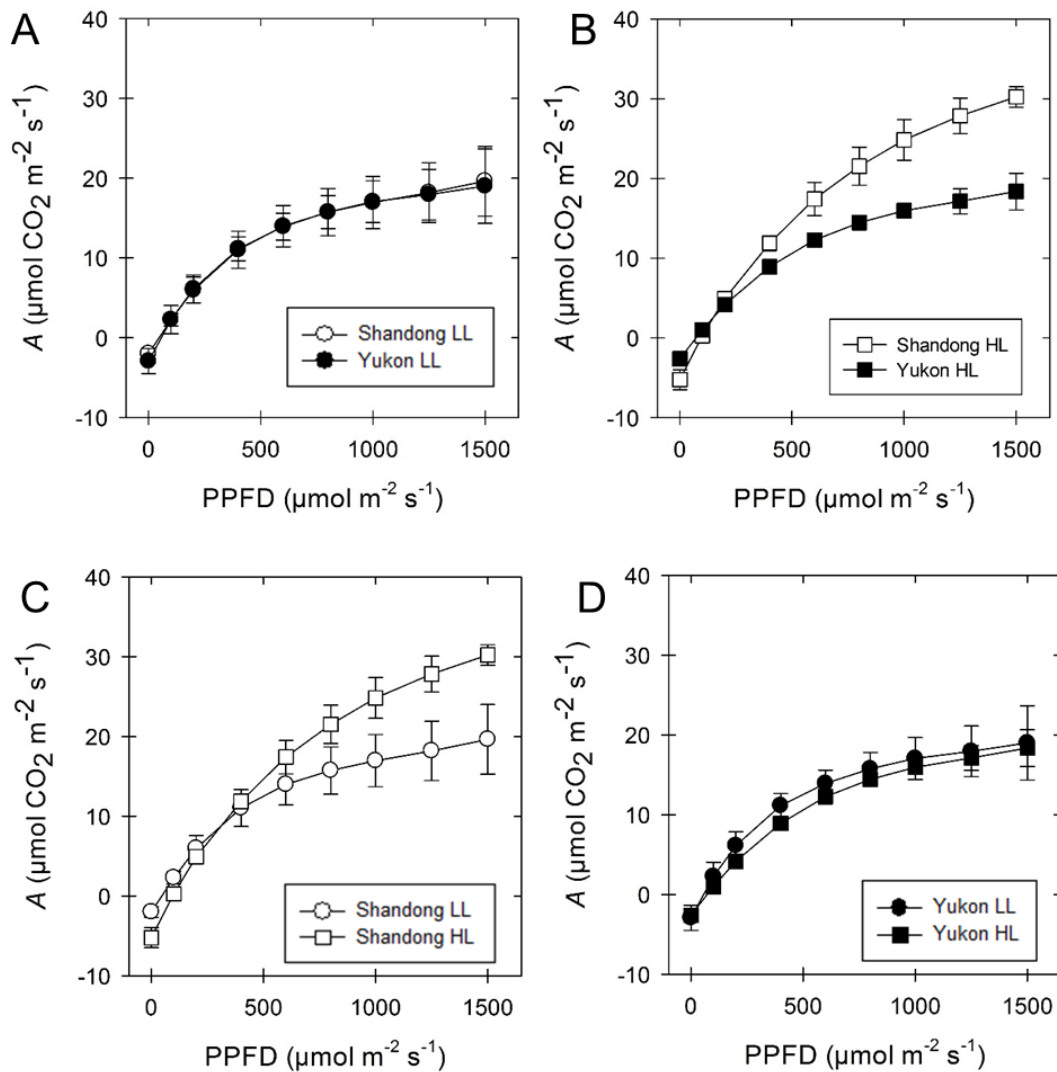


Figure 4.11. Light-response curves at 800 C_a for the Shandong and Yukon ecotypes of *Eutrema* developed at different growth irradiance. Plants of each ecotype were grown under either 250 (LL) or 750 $\mu\text{mol photons m}^{-2} \text{ s}^{-1}$ (HL) PPFD. Light was set up in 9 steps (1500, 1250, 1000, 800, 600, 400, 200, 100, 0 $\mu\text{mol photons m}^{-2} \text{ s}^{-1}$), leaf temperature was maintained at 22°C and relative humidity 50-80%. Shandong LL (○); Yukon LL (●); Shandong HL (□); Yukon HL (■). Ecotypic comparison under LL (A) and HL (B) conditions. Growth irradiance comparisons for the Shandong (C) and Yukon (D) ecotypes. Values represent means \pm SE ($n = 6$ to 8). HL, high-light; LL, low-light; PPFD, photosynthetic photon flux density; SE, Standard error.

Table 4.4 Photosynthetic parameters derived from light-response curves of the Shandong and Yukon ecotypes of *Eutrema* growth under two different irradiance. Plants of each ecotype were grown under either 250 (LL) or 750 $\mu\text{mol photons m}^{-2} \text{s}^{-1}$ (HL) PPFD. Light-response curves were constructed at 200 C_a and 9 light steps (0 - 1500 $\mu\text{mol photons m}^{-2} \text{s}^{-1}$). Photosynthetic parameters were modelled using an analysis software. The data was analyzed using a two-way ANOVA and a multiple comparison test was done using the Holm-Sidak method Values represent means \pm SE ($n = 5$ to 8). A_{max} , maximal rate of CO_2 uptake; ANOVA, analysis of variance; C_a , ambient CO_2 ; HL, high-light; LL, low-light; PPFD, photosynthetic photon flux density; R_{dark} , rate of dark respiration; SE, standard error.

Ecotype and Growth irradiance	A_{max} ($\mu\text{mol CO}_2 \text{ m}^{-2} \text{ s}^{-2}$)	$\Phi_{\text{app CO}_2}$ ($\mu\text{mol CO}_2 \text{ photons m}^{-2} \text{ s}^{-1}$)	Light compensation point ($\mu\text{mol photons m}^{-2} \text{ s}^{-1}$)	R_{dark} ($\mu\text{mol CO}_2 \text{ m}^{-2} \text{ s}^{-1}$)	Light saturation estimate ($\mu\text{mol photons m}^{-2} \text{ s}^{-1}$)
Shandong LL	9.11 ± 0.90^b	0.0393 ± 0.00696^a	77.34 ± 12.21^a	-2.98 ± 0.62^b	336.57 ± 35.50^{bc}
Yukon LL	10.40 ± 1.25^b	0.0572 ± 0.0129^a	95.88 ± 12.68^a	-4.88 ± 0.76^a	302.17 ± 34.98^c
Shandong HL	12.92 ± 0.76^a	0.0414 ± 0.0374^a	103.26 ± 8.47^a	-4.22 ± 0.33^b	421.00 ± 30.31^{ab}
Yukon HL	8.13 ± 0.42^b	0.0234 ± 0.00176^b	105.76 ± 10.41^a	-2.48 ± 0.30^c	463.25 ± 25.00^a

under LL conditions ($P = 0.003$). A statistically significant interaction was found between ecotype and growth irradiance ($P = 0.022$).

The light compensation point from the light response curves shows that plants grown under HL conditions have higher light compensation points but there is not a statistically significant interaction between ecotype and growth ($P = 0.496$) (Table 4.4).

The rates of dark respiration showed that under LL and HL conditions there is a difference when an ecotypic comparison is made ($P = 0.020$ and $P = 0.035$). However, even though the Shandong ecotype shows an increase in the dark respiration rate no statistically significant difference was found ($P = 0.133$). Interestingly, the Yukon ecotype shows the opposite trend as the Shandong with lower dark respiration rates when grown under HL conditions and a statistically significant difference was found ($P = 0.004$). (Table 4.4). No statistically significant interaction was found between ecotype and growth irradiance ($P = 0.496$).

Light saturation estimate shows that there is no difference between the two ecotypes when grown under LL conditions ($P = 0.451$). Both ecotypes increase the light saturation estimate when grown under HL conditions and no difference was found either ($P = 0.368$). Under HL conditions there is an increase in the light saturation estimate for the two ecotypes. When the Yukon ecotype was compared for the two growth irradiances a significant difference was found ($P = 0.001$). Despite the fact that there is an increase in the light saturation estimate there are no differences for the Shandong ecotype grown under LL and HL conditions ($P = 0.087$) (Table 4.4). No statistically significant interaction was found between ecotype and growth irradiance ($P = 0.245$).

4.3.1.2 Photosynthetic Derived Parameters at 400 C_a

A_{\max} modelled values derived from the light response curves done with an ambient level of 400 C_a shows that the Shandong ecotype grown under HL conditions has the highest rate of A_{\max} and a difference was found compared to the Shandong plants grown under LL conditions ($P \leq 0.001$) and with the Yukon ecotype under HL conditions ($P \leq 0.001$). The Yukon ecotype does not exhibit differences in the maximum photosynthetic rate irrespective of the growth irradiance that is grown ($P = 0.945$) (Table

4.5). A statistically significant interaction was found between ecotype and growth irradiance ($P = 0.011$).

The $\Phi_{\text{app}} \text{CO}_2$ yield of shows that the only difference found was for the two ecotypes grown under HL conditions ($P = 0.033$). No difference was found under LL conditions when the two ecotypes were compared ($P = 0.400$). The Shandong ecotype increases the $\Phi_{\text{app}} \text{CO}_2$ when is grown under HL but no difference was found between plants grown under the two regimes ($P = 0.188$). Conversely, the Yukon ecotype decreases the $\Phi_{\text{app}} \text{CO}_2$ when grown under an increased irradiance. However, no difference were found ($P = 0.071$) (Table 4.5). A statistically significant interaction was found between ecotype and growth irradiance ($P = 0.032$).

The light compensation point shows that there is not a statistically significant interaction between ecotype and growth ($P = 0.109$) (Table 4.5).

The calculated dark respiration rates showed that the Shandong ecotype grown under HL conditions has the highest dark respiration rate and there is a difference when compared to the Yukon ecotype grown under the same conditions ($P = 0.011$) and the Shandong plants grown under LL conditions ($P = 0.034$). The Yukon exhibits the opposite trend as the Shandong ecotype and decreases the dark respiration rates when grown under HL conditions, but no difference was found between the two light regimes ($P = 0.125$). (Table 4.5). A statistically significant interaction was found between ecotype and growth irradiance ($P = 0.011$).

The light saturation estimate shows an increase for the plants grown under HL conditions. The Yukon ecotype shows the biggest increase when a comparison was made within this ecotype and there is a significant difference between Yukon plant grown under LL and HL conditions ($P = 0.014$). However, no difference was found when the same comparison was made in the Shandong ecotype despite the increase ($P = 0.125$). No differences were found for the two ecotypes grown under LL ($P = 0.372$) or HL conditions ($P = 0.931$) (Table 4.5). No statistically significant interaction was found between ecotype and growth irradiance ($P = 0.600$).

Table 4.5 Photosynthetic parameters derived from light-response curves of the Shandong and Yukon ecotypes of *Eutrema* growth under two different irradiance. Plants of each ecotype were grown under either 250 (LL) or 750 $\mu\text{mol photons m}^{-2} \text{s}^{-1}$ (HL) PPFD. Light-response curves were constructed at 400 C_a and 9 light steps (0 - 1500 $\mu\text{mol photons m}^{-2} \text{s}^{-1}$). The data was analyzed using a two-way ANOVA and a multiple comparison test was done using the Holm-Sidak method. Different letters within columns indicate a significant difference at $P = 0.05$. Values represent means \pm SE ($n = 6$ to 10). A_{max} , maximal rate of CO_2 uptake; ANOVA, analysis of variance; C_a , ambient CO_2 ; HL, high-light; LL, low-light; PPFD, photosynthetic photon flux density; R_{dark} , rate of dark respiration; SE, standard error.

Ecotype and Growth irradiance	A_{max} ($\mu\text{mol CO}_2 \text{ m}^{-2} \text{ s}^{-2}$)	$\Phi_{\text{app CO}_2}$ ($\mu\text{mol CO}_2 \text{ photons m}^{-2} \text{ s}^{-1}$)	Light compensation point ($\mu\text{mol photons m}^{-2} \text{ s}^{-1}$)	R_{dark} ($\mu\text{mol CO}_2 \text{ m}^{-2} \text{ s}^{-1}$)	Light saturation estimate ($\mu\text{mol photons m}^{-2} \text{ s}^{-1}$)
Shandong LL	17.34 \pm 1.35 ^b	0.0384 \pm 0.00426 ^a	69.72 \pm 12.49 ^a	-2.49 \pm 0.35 ^b	519.67 \pm 58.44 ^{ab}
Yukon LL	16.66 \pm 1.19 ^b	0.0452 \pm 0.00522 ^{ab}	77.27 \pm 9.11 ^a	-3.52 \pm 0.63 ^b	452.90 \pm 59.00 ^b
Shandong HL	25.35 \pm 2.80 ^a	0.0507 \pm 0.0118 ^a	92.35 \pm 9.50 ^a	-5.09 \pm 1.80 ^a	652.83 \pm 57.12 ^a
Yukon HL	16.52 \pm 0.89 ^b	0.0303 \pm 0.00388 ^b	65.71 \pm 8.21 ^a	-1.92 \pm 0.25 ^b	645.44 \pm 39.66 ^a

4.3.1.3 Photosynthetic Derived Parameters at 800 C_a

The results from the data modelling for A_{\max} done with an ambient concentration of 800 C_a exhibit the same trend as the results done with an ambient level of 400 C_a. The Shandong ecotype grown under HL conditions has the highest A_{\max} and a statistically significant difference was found when compared to the Yukon under the same conditions ($P \leq 0.001$) and when compared to the Shandong plants grown under LL conditions ($P \leq 0.001$). Interestingly, the Yukon ecotype does not increase the maximum photosynthetic rates as Shandong does, no difference was found for this ecotype grown under LL and HL conditions ($P = 0.239$). (Table 4.6). A statistically significant interaction was found between ecotype and growth irradiance ($P = 0.010$).

Φ_{app} CO₂ yield exhibits very similar values between ecotypes irrespective of the growth irradiance. There is not a statistically significant interaction between ecotype and growth ($P = 0.606$) (Table 4.6).

The light compensation point shows that the difference in the mean values among ecotypes and there is not a statistically significant interaction between ecotypes and growth irradiance ($P = 0.103$) (Table 4.6).

Rates of dark have very similar rates for both ecotypes under the two growing conditions. There is not a statistically significant interaction between ecotypes and growth irradiance ($P = 0.098$). (Table 4.6).

The calculated light saturation estimate shows an increase for the plants grown under HL conditions. Under LL conditions there is no statistically significant difference between the two ecotypes ($P = 0.505$). As mentioned before there is an increase when plants were grown under HL conditions with a higher increase in the LSE for the Shandong ecotype than the Yukon and a significant difference was found ($P = 0.024$). When a comparison was made within ecotypes a significant difference was found for the Shandong ecotype under the two light conditions ($P \leq 0.001$). Same trend was found for the Yukon ecotype ($P \leq 0.001$) (Table 4.6). No statistically significant interaction was found between ecotype and growth irradiance ($P = 0.171$).

Table 4.6 Photosynthetic parameters derived from light-response curves of the Shandong and Yukon ecotypes of *Eutrema* growth under two different irradiance. Plants of each ecotype were grown under either 250 (LL) or 750 $\mu\text{mol photons m}^{-2} \text{s}^{-1}$ (HL) PPFD. Light-response curves were constructed at 800 C_a and 9 light steps (0 - 1500 $\mu\text{mol photons m}^{-2} \text{s}^{-1}$). The data was analyzed using a two-way ANOVA and a multiple comparison test was done using the Holm-Sidak method. Different letters within columns indicate a significant difference at $P = 0.05$. Values represent means \pm SE ($n = 4$ to 8). A_{max} , maximal rate of CO_2 uptake; ANOVA, analysis of variance; HL, high-light; LL, low-light; PPFD, photosynthetic photon flux density; C_a , ambient CO_2 ; R_{dark} , rate of dark respiration; SE, standard error.

Ecotype and Growth irradiance	A_{max} ($\mu\text{mol CO}_2 \text{ m}^{-2} \text{ s}^{-2}$)	$\Phi_{\text{app CO}_2}$ ($\mu\text{mol CO}_2 \text{ photons m}^{-2} \text{ s}^{-1}$)	Light compensation point ($\mu\text{mol photons m}^{-2} \text{ s}^{-1}$)	R_{dark} ($\mu\text{mol CO}_2 \text{ m}^{-2} \text{ s}^{-1}$)	Light saturation estimate ($\mu\text{mol photons m}^{-2} \text{ s}^{-1}$)
Shandong LL	28.13 \pm 3.12 ^b	0.0536 \pm 0.00698 ^a	40.16 \pm 4.24 ^a	-2.14 \pm 0.38 ^a	582.50 \pm 34.40 ^c
Yukon LL	26.04 \pm 3.02 ^b	0.0533 \pm 0.00587 ^a	57.17 \pm 14.18 ^a	-2.98 \pm 0.92 ^a	552.00 \pm 33.04 ^c
Shandong HL	54.78 \pm 1.05 ^a	0.0489 \pm 0.00566 ^a	72.10 \pm 4.97 ^a	-3.60 \pm 0.65 ^a	933.00 \pm 44.66 ^a
Yukon HL	31.83 \pm 4.28 ^b	0.0420 \pm 0.0461 ^a	57.66 \pm 6.67 ^a	-2.32 \pm 0.29 ^a	803.88 \pm 26.10 ^b

4.3.1.4 Water use efficiency

Intrinsic WUE results showed no ecotypic difference when a comparison was made under LL and HL. A comparison between the two growth irradiance showed no difference in the Shandong ecotype under LL and HL conditions ($P = 0.360$). However, the Yukon ecotype showed an increase WUE when it was grown under HL conditions and a comparison made between LL and HL growth conditions showed a statistically significant difference ($P = 0.012$).

4.3.2 CO₂ Responses

Photosynthesis rates were determined through a CO₂ response curve for each growing condition (LL and HL) for both the Shandong and Yukon ecotypes of *Eutrema*. The measurements were done as described in 3.3.2.

The CO₂ response curve for the Shandong and Yukon ecotype grown under LL conditions exhibits a very similar trend with minimal differences (Fig. 4.12A). For plants grown under HL conditions the Shandong ecotype exhibits a higher response to increasing levels of CO₂ compared to the Yukon ecotype showing higher rates of net photosynthesis even with low ambient concentrations of CO₂ (Fig. 4.12B).

A comparison between the two growth irradiances (LL and HL) for the Shandong ecotype of the CO₂ response curve shows that the plants grown under HL exhibit a higher net photosynthetic response to increased ambient CO₂ levels when compared to plants grown under LL conditions (Fig. 4.12C). The CO₂ response for the Yukon ecotype grown under LL and HL conditions exhibits a similar trend and the differences are minimal between these two growing conditions (Fig. 4.12D).

A_{\max} values modelled from the CO₂ response curves shows that the Shandong ecotype grown under HL conditions has the higher maximum photosynthetic rates. There is trend towards an increase A_{\max} for plants grown under HL conditions. There is no statistically significant difference between the two ecotypes grown under LL conditions ($P = 0.582$). As mentioned before plants grown under HL conditions display higher rates of photosynthesis particularly the Shandong ecotype and in a lesser extent the Yukon ecotype and no difference was found between them ($P = 0.134$). Despite the increase rates under HL conditions for the Yukon ecotype there is no statistically

Table 4.7 Intrinsic water use efficiency of the Shandong and Yukon ecotypes of *Eutrema* grown under either 250 (LL) or 750 $\mu\text{mol photons m}^{-2} \text{s}^{-1}$ (HL) PPFD. WUE was determined at an irradiance of 200 and 800 $\mu\text{mol photons m}^{-2} \text{s}^{-1}$ for LL and HL growth conditions, respectively. All measurements were determined at 400 C_a . Values represent means \pm SE ($n = 5$ to 10). Different letters indicate a significant difference at $P = 0.05$ based on a two-way ANOVA. ANOVA, analysis of variance; HL, high-light; LL, low-light; PPFD, photosynthetic photon flux density; SE, standard error; WUE, water use efficiency.

Ecotype	Growth irradiance	WUE ($\mu\text{mol CO}_2 \text{ mmol H}_2\text{O}^{-1}$) 200 and 800 ($\mu\text{mol photons m}^{-2} \text{s}^{-1}$)
Shandong	LL	0.79 ± 0.39^b
Yukon	LL	0.65 ± 0.12^b
Shandong	HL	1.35 ± 0.46^{ab}
Yukon	HL	1.93 ± 0.34^a

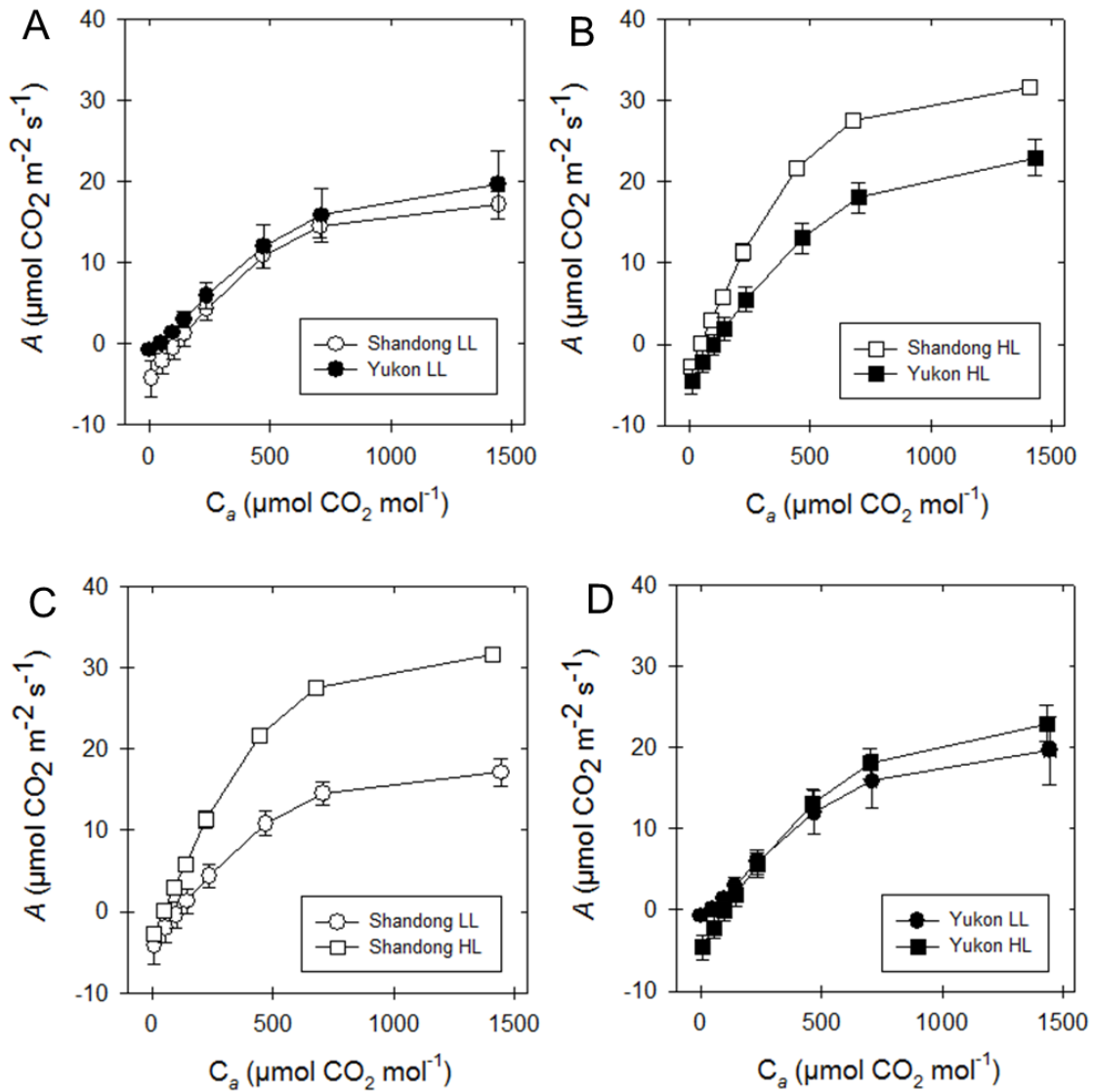


Figure 4.12 CO₂-response curves for the Shandong and Yukon ecotypes of *Eutrema* developed at different growth irradiance (LL and HL). Plants of each ecotype were grown under either 250 (LL) or 750 μmol photons m⁻² s⁻¹ (HL) PPFD. CO₂-response curves were constructed at a saturating PPFD of 1500 μmol photons m⁻² s⁻¹. C_a was set up in 8 steps (0 – 1500 μmol CO₂ mol⁻¹). Shandong LL (○); Yukon LL (●); Shandong HL (□); Yukon HL (■). Ecotypic comparison under LL (A) and HL (B) conditions. Growth irradiance comparisons for the Shandong (C) and Yukon (D) ecotypes. Values represent means ± SE (*n* = 6 to 12). C_a, Ambient CO₂ level; HL, high-light; LL, low-light; PPFD, photosynthetic photon flux density; SE, Standard error.

Table 4.8. Photosynthetic parameters derived from CO₂-response curves of Shandong and Yukon ecotypes growth under two different irradiance. Plants of each ecotype were grown under either 250 (LL) or 750 $\mu\text{mol photons m}^{-2} \text{s}^{-1}$ (HL) PPFD. CO₂-response curves were constructed at a saturating PPFD of 1500 $\mu\text{mol photons m}^{-2} \text{s}^{-1}$. Photosynthetic parameters were modelled using an analysis software. The data was analyzed using a two-way ANOVA and a multiple comparison test was done using the Holm-Sidak method. Different letters within columns indicate a significant difference at $P = 0.05$. Values represent means \pm SE ($n = 6$ to 12). A_{max} , maximal rate of CO₂ uptake; ANOVA, analysis of variance; C_a , ambient CO₂ level; CE, carboxylation efficiency; Γ^* , CO₂ compensation point; HL high-light; LL, low-light; PPFD, photosynthetic photon flux density; SE, standard error.

Ecotype and growth irradiance	A_{max} ($\mu\text{mol CO}_2 \text{ m}^{-2} \text{ s}^{-1}$)	CE ($\mu\text{mol m}^{-2} \text{ s}^{-1}$)	Γ^* ($\mu\text{mol mol}^{-1}$)	Respiration ($\mu\text{mol CO}_2 \text{ m}^{-2} \text{ s}^{-1}$)
Shandong LL	29.80 \pm 2.88 ^b	0.0382 \pm 0.00624 ^b	93.40 \pm 18.84 ^a	-4.94 \pm 1.22 ^a
Yukon LL	33.26 \pm 3.55 ^b	0.0268 \pm 0.0540 ^b	37.27 \pm 8.51 ^c	-1.86 \pm 0.22 ^a
Shandong HL	51.79 \pm 3.84 ^a	0.0639 \pm 0.00906 ^a	48.30 \pm 1.26 ^{bc}	-4.68 \pm 0.46 ^a
Yukon HL	42.75 \pm 5.81 ^{ab}	0.0510 \pm 0.00776 ^a	86.94 \pm 15.38 ^{ab}	-5.92 \pm 1.44 ^a

significant difference when plants of this ecotype are compared between the two light regimes ($P = 0.158$). The Shandong ecotypes shows a higher increase for plants grown under HL than the Yukon ecotype and there is a significant difference for Shandong plants grown under LL and HL ($P \leq 0.001$) (Table 4.8). No statistically significant interaction was found between ecotype and growth irradiance ($P = 0.154$).

The calculated carboxylation efficiency shows a trend towards increased values for plants grown under HL than plants grown under LL conditions for the two ecotypes. However, no statistically significant difference was found for plants of the two ecotypes under LL and HL conditions ($P = 0.319$ and $P = 0.230$). The ecotypic comparison showed that the Shandong ecotype exhibit statistically significant difference when grown under LL and HL conditions ($P = 0.014$). The same trend was observed for the Yukon ecotype and a significant difference was found under the two light regimes ($P = 0.050$) (Table 4.8). No statistically significant interaction was found between ecotype and growth irradiance ($P = 0.918$).

The CO₂ compensation point show a different trend between the two ecotypes. Shandong has a decrease in the CO₂ compensation point for plants grown under HL conditions respect the plants grown under LL. Conversely, Yukon has an increase when plants are grown under HL conditions. Therefore, a statistically significant difference was found in plants of both ecotypes grown under LL conditions ($P = 0.019$). Despite the different trend in between the two ecotypes no significant difference was found for plants grown under HL conditions ($P = 0.081$). The ecotypic comparison shows that there is a statistically significant difference for the Shandong ecotype under LL and HL conditions ($P = 0.032$). Also a significant difference was found for the Yukon ecotype under the two light regimes ($P = 0.046$) (Table 4.8). A statistically significant interaction was found between ecotype and growth irradiance ($P = 0.005$).

Rates of respiration in the light results showed that the effect of the ecotypes is not dependent on the level of growth irradiance and there is not a statistically significant interaction between ecotype and growth irradiance ($P = 0.071$) (Table 4.8). No statistically significant interaction was found between ecotype and growth irradiance ($P = 0.071$).

These results suggest that the Yukon ecotype is less responsive to the different growth conditions than Shandong.

4.4 Photoinhibition of Photosynthesis

The exposure of detached leaves of *Eutrema* from Shandong and Yukon ecotypes grown under LL (250 $\mu\text{mol photons m}^{-2}\text{s}^{-1}$) light conditions to a saturated irradiance of 1750 $\mu\text{mol photons m}^{-2}\text{s}^{-1}$ and under a low temperature (2°C) showed different levels of photoinhibition between the two ecotypes examined.

For the plants grown under LL conditions Shandong exhibits a higher susceptibility to photoinhibition with a reduction on F_v/F_m of 78%, while Yukon showed a reduction of 50% F_v/F_m as showed in Fig. 4.13.

Plants grown under HL conditions exhibit the same trend as LL plants. Shandong has a higher susceptibility than Yukon to photoinhibition. However, both ecotypes are less susceptible than plants grown under LL. The F_v/F_m in Shandong was 64% and Yukon had a reduction of 11% (Fig. 4.13). Regardless the growth conditions of Yukon this ecotype shows a higher tolerance to photoinhibition than Shandong. Increased growth irradiance appears to play an important role increasing the tolerance of both ecotypes to photoinhibition, particularly in Yukon and in a lesser extent in Shandong. Pre-photoinhibition no significant difference was found between the two ecotypes under LL conditions ($P = 0.278$). However, under HL conditions there was a statistically significant difference between the two ecotypes ($P < 0.001$). Also a significant difference was found pre-photoinhibition between the two growth conditions of Shandong ($P < 0.001$). Post-photoinhibition results showed a statistically significant difference between the two growth irradiance and ecotypes ($P < 0.001$). A statistically significant difference was found for each ecotype under both growth conditions between pre-photoinhibition and post-photoinhibition ($P < 0.001$).

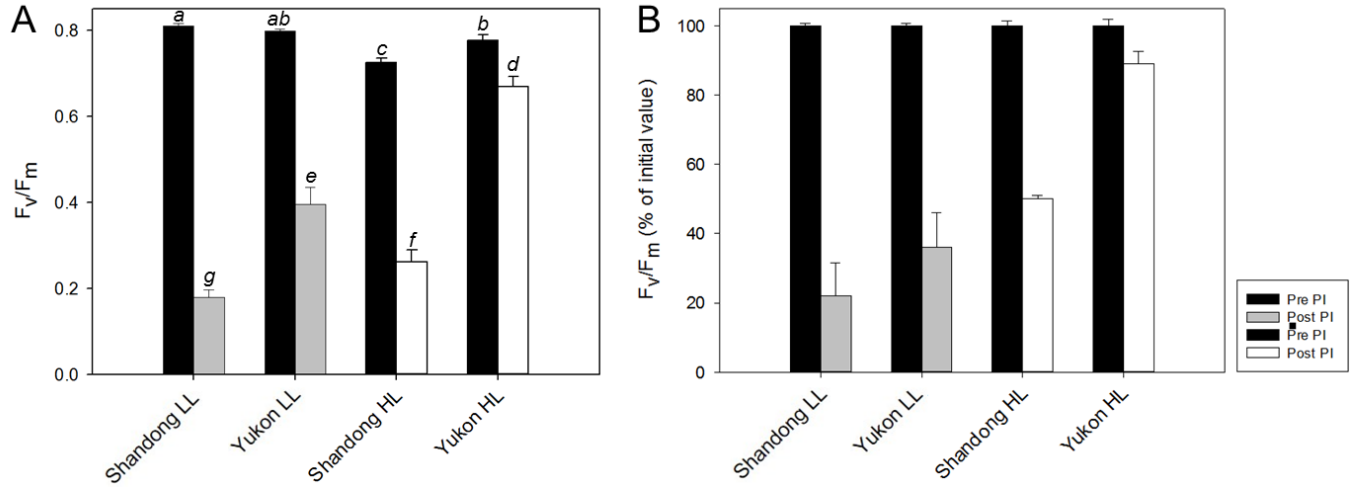


Figure 4.13 Photoinhibition of photosynthesis for the Shandong and Yukon ecotypes of *Eutrema* developed at different growth irradiances. Plants of each ecotype were grown under either 250 (LL) or 750 $\mu\text{mol photons m}^{-2} \text{s}^{-1}$ (HL) PPFD. Detached leaves were exposed to 1750 $\mu\text{mol photons m}^{-2} \text{s}^{-1}$ for 2 hours at 2°C and responses determined by monitoring changes in the F_v/F_m ratio. Black bars represent pre-photoinhibition and are compared to post-photoinhibition for LL (grey bars) and HL (white bars) grown material of each ecotype. Actual F_v/F_m values (**A**) and normalized F_v/F_m (**B**) are presented. The data was analyzed using a one-way ANOVA and a multiple comparison test was done using the Holm-Sidak method. Different letters indicate a significant difference at $P = 0.05$. Values represent means \pm SD ($n = 8$). ANOVA, analysis of variance; F_m , maximal fluorescence in the dark-adapted state; F_v , variable fluorescence in the dark-adapted state; F_v/F_m , maximal quantum efficiency of PSII; HL, high-light; LL, low-light; PPFD, photosynthetic photon flux density; PSII, photosystem II; SD, standard deviation.

CHAPTER 5

5.0 Discussion

5.1 Responses to Growth Irradiance

5.1.1 Shandong: A Tough Resilient Plant

Some results at a chloroplast level for the Shandong ecotype were not as expected when grown under HL conditions. Results from total chlorophyll on a FW shows a 16% decrease for plants grown under HL and when calculated on an area basis the trend is towards a 22% increase under the same conditions this response is the expected according to photoacclimation to growth irradiance previously observed (Anderson 1986; Anderson and Osmond 1987). Total carotenoid contents tend to increase when the plants are under HL, these findings have been observed previously as carotenoids play a role preventing photooxidation and are involved in the dissipation of excess of energy through NPQ (Demmig-Adams and Adams 1992). However, where this ecotype showed an interesting non-typical response was in anthocyanin contents. Anthocyanin accumulation on this ecotype is lower for plants grown under HL than for plants grown under LL conditions, and these results are opposed as the reported in the literature (Kimura et al. 2003). The most shocking result found at a chloroplast level for the Shandong ecotype was Chl *a:b* ratio. Chl *a:b* ratio is one reliable indicator of low-high light photoacclimation, typically LL plants have lower values than HL plants (Anderson 1986; Anderson and Osmond 1987). Interestingly, the Shandong ecotype does not modify Chl *a:b* ratio in response to high irradiance. Chow et al. (1991) showed that *Tradescantia albiflora* (Kunth) does not modify Chl *a:b* ratio when is grown under HL conditions.

Leaf level changes were assessed through growth kinetics. Sampling points were determined by FW accumulation and those results are correlated with DW, total leaf area, and leaves number. Shandong plants are approximately at the same developmental stage when LL plants are 27 days and HL plants 24 days old. Initial development is very similar, and then HL plants grew at a faster rate than LL plants. RGR results are consistent with the absolute growth measurements, HL plants displayed 1.2-fold increase in the same interval compared to LL plants. Growth kinetics

results can be correlated with typical low and high light leaf-level photoacclimation in many species (Boardman 1977; Givnish 1988).

Whole plant level photoacclimation was studied through gas exchange. Light-response curves done with three different ambient CO₂ levels were performed. Low ambient CO₂ or photorespiratory conditions, reference ambient CO₂ and high ambient CO₂ levels which are proper conditions to suppress photorespiration. The light-response curve done with low CO₂ (200 C_a) shows a typical low-high light plant response. Same results were obtained when the curves were done with a reference ambient CO₂ level (400 C_a) and under non-photorespiratory conditions (800 C_a). A typical LL-HL response was observed with higher maximum photosynthetic rates, higher light compensation point, higher dark respiration rates and an increased light saturation estimate for plants grown under HL. These results are consistent with the reported low-high light photoacclimation responses in different species (Anderson and Osmond 1987). CO₂- and light-response curves for the Shandong ecotype are the expected for HL plants reported previously by Anderson and Osmond (1987).

Photoacclimated Shandong plants exhibit high photosynthetic rates probably due to higher carboxylation rates, increased electron transport capacity and increased Rubisco contents as reported in *Arabidopsis* grown in high light by Bailey et al. (2004). Similar results were reported in pea plants by Evans (1987). Typically a strong correlation is suggested between maximum photosynthetic rates and Chl *a:b* as an indication of photoacclimation. This ecotype demonstrates that this mechanisms appear to act independently and confirms the hypothesis of Bailey et al. (2001) that these mechanisms act independently but are triggered by the same responses. Tolerance to photoinhibition showed that plants grown under LL conditions are more susceptible and F_v/F_m decreased 78% and 64% for plants grown under LL and HL respectively. Growth under high irradiance increases the tolerance to photoinhibition in this ecotype and these results have been reported previously in other species (Anderson and Osmond 1987; Anderson et al. 1995). This ecotype appears to acclimate to HL conditions modulating the carbon metabolism, mainly by suppressing photorespiration. I hypothesize that another protective mechanism that might be involved is the PTOX. Lennon et al. (2003) found that the abundance and activity of PTOX is very low in

mature leaves of C3 plants and as an exception to the rule Streb et al. (2005) demonstrated that the high mountain plant *Ranunculus glacialis* has high contents of PTOX in fully developed leaves that allow this plant to maintain high photosynthetic electron capacity under HL and low temperatures. Stepien and Johnson (2009) also found increased contents of PTOX in mature leaves of Shandong in response to salt stress. I hypothesize that Shandong might be using the PTOX as an alternative electron sink to acclimate to high irradiance. However, the function of this enzyme have been controversial. Rosso et al. (2006) found that PTOX does not act as a photoprotective mechanism when plants are exposed to high irradiance.

5.1.2 Yukon: A High-Light Loving Plant

At a chloroplast level in this ecotype the main changes in pigment composition showed that total chlorophyll on a FW basis displayed a decrease of 37% for the plants grown under HL conditions, Chl *a:b* ratio had an increase of approximately 1.9-fold. These responses resemble previous results observed for growth irradiance photoacclimation (Anderson 1986; Schötler and Toth 2014). Total carotenoids on a FW basis does not show any difference. However, on an area basis there is an increase when plants were grown under high irradiance and as mentioned previously these pigments play an important role in energy dissipation through NPQ (Demmig-Adams and Adams 1992). Other key pigment that act as a protective mechanism is anthocyanin. Anthocyanin accumulation on a FW basis showed a 1.3-fold increase for plants grown under HL. Anthocyanin is reported to protect mesophyll cells against excess of irradiance through light attenuation also as an antioxidant (Krol et al. 1996; Chalker-Scott 1999; Neill and Gould 2003; Gould 2004).

The different growth irradiances used on this study resulted in different developmental rates of the plants. FW accumulation was used to determine the same developmental stage between LL and HL plants. Plants were harvested approximately 22 and 23 days after seeding. FW and DW measurements displayed the same trend but towards the end of the examined cycle plants grown under HL accumulated a higher mass and these results are reported in the literature for low-high light responses (Givnish 1988). SLA values for plants grown under LL indicates that these plants have

thinner leaves than the plants under HL. Thicker leaves have an increased mesophyll volume that allows a better diffusion of CO₂ that optimizes photosynthetic rates (Terashima et al. 2006). RGR confirms the other analyzed traits showing that the differences between growth irradiances are minimal. It appears that the Yukon ecotype does not respond as many species even with 1.5-fold higher PPFD probably indicating that the tolerance to light stress is higher than many species and requires high irradiance to display the typical LL and HL differences (Boardman 1977; Givnish 1988).

CO₂- and light- response curves exhibit minimal differences when plants were grown under LL and HL conditions. Interestingly, this ecotype appears to modulate the photorespiratory processes as a photoacclimation mechanism to the increased growth irradiance. Previous research done in this laboratory demonstrated that Yukon is not able to grow and/or complete its life cycle under low light conditions (100 μmol photons m⁻² s⁻¹) and this might be owed to respiratory losses (Khanal 2011). This condition is probably associated to the stressful environmental conditions that these plants grow investing energy in respiration as a protective mechanism (Chapin III et al. 1993; Block et al. 2009).

Tolerance to photoinhibition showed that plants grown under LL conditions are more susceptible and F_v/F_m decreased 50% and 11% for plants grown under LL and HL respectively. Growth under high irradiance increases the tolerance to photoinhibition in this ecotype and these results have been reported previously in other species (Anderson and Osmond 1987; Anderson et al. 1995). As the results indicate Yukon seems to acclimate to high irradiance by modifying its pigment composition and using photorespiration as a protective mechanism. Huang et al. (2014) demonstrated in tobacco that photorespiration is necessary to maintain high photosynthetic rates under increased growth irradiance scavenging 2-PG combining two molecules to yield 3-PGA preventing the accumulation of 2-PG and other photorespiratory intermediates helping to maintain high rates of photosynthesis. Timm et al. (2012) found that the overexpression of the H-protein of glycine decarboxylase one of the main enzymes of photorespiration leads to increased photosynthetic rates in *Arabidopsis*. Another interesting conclusion from Kozaki and Takeba (1999) is that photorespiration acts as a protective mechanism against photoinhibition. It appears that the Yukon ecotype has

adapted to its natural environment mainly modulating its carbon metabolism and using photorespiration as a sink to avoid damages to the photosynthetic apparatus. Other proposed protective mechanism is ureide accumulation. Malik et al. (2015) reported ureide accumulation in leaf tissue of the Yukon ecotype of *Eutrema* grown under HL and this accumulation is directly related with an increase in the photoinhibition tolerance of this ecotype under HL conditions.

5.2 Contrasting Results Between Ecotypes Acclimated to High-Light

At a chloroplast level the contrasting response of the two analysed ecotypes of *Eutrema* are Chl *a:b* ratio and anthocyanin contents. Anthocyanin contents for Shandong are lower than Yukon and probably that lower accumulation in Shandong can be correlated with a higher susceptibility to photoinhibition. Chl *a:b* ratios showed a typical low-high light photoacclimation response in Yukon. Conversely, Shandong shows a constant ratio. Chow et al. (1991) obtained similar results with *Tradescantia albiflora* a constant Chl *a:b* ratio when plants were grown under LL or HL, this inflexibility makes *Tradescantia* prone to photoinhibition. Results from the photoinhibition experiment demonstrated that Shandong experiences a decrease in F_v/F_m of 64% while Yukon had a reduction of 11%. I hypothesize that the contrasting results obtained at a chloroplast level are the probable reasons that Shandong is more susceptible to photoinhibition than Yukon.

At leaf level the contrasting differences are not as determinant as when a comparison was made on a chloroplast level. The first two weeks of development Yukon appears to grow at a slightly higher rate than Shandong. However, after that initial period Shandong grows at a faster rate than Yukon. Those results are represented in the growth kinetics experiment results. Light-response curves done with plants of the two ecotypes grown under HL conditions showed that the Shandong ecotype appears to have a superior photosynthetic performance than the Yukon ecotype. According to the gas exchange results at a whole plant level the response is a lack of photorespiration vs. photorespiration for Shandong and Yukon respectively. Tolerance to photoinhibition shows that Shandong is not as capable to withstand high-irradiance and low temperatures as Yukon.

5.3 Conclusions and Future Work

The contrasting natural environment of the Shandong and the Yukon ecotypes of *Eutrema* influences the different response mechanisms of these ecotypes to the increased growth irradiance. Photosynthesis is a very effective environmental sensor mechanism and is highly sensitive to any imbalance. To photoacclimate plants have evolved a myriad of mechanisms. This study demonstrated that these ecotypes exhibit different photoacclimation mechanisms to growth irradiance.

The Shandong ecotype shows an interesting trend at chloroplast level, no changes were observed in the Chl *a*:*b* when plants of this ecotype were grown under HL conditions. Anthocyanin contents for Shandong also showed a non-typical response with lower contents for plants grown under HL than plants under LL conditions. At a whole plant level light-response curves showed a typical low- high-light response. Plants of this ecotype grown under HL had higher maximum photosynthetic rates, higher light compensation point and light saturation estimate than plants grown under LL conditions. Tolerance to photoinhibition is increased when plants of Shandong were grown under HL compared to plants grown under LL conditions. However, photoinhibition tolerance is lower in Shandong when compared to Yukon under both growing conditions. The results from this study showed that the Shandong ecotype of *Eutrema* appears to acclimate to high irradiance suppressing photorespiration and probably using PTOX as an alternative electron sink to dissipate the excess of energy.

The Yukon ecotype appears to have the typical response of low- high-light plants at a chloroplast level with the total chlorophyll levels on a FW basis showing a decrease when growth irradiance was increased and Chl *a*:*b* ratio also showing an increase for plants grown under HL when compared to plants grown under LL conditions. At a leaf level Yukon plants showed minimal differences with plants of this same ecotype grown under LL and HL conditions. Gas exchange measurements showed that this ecotype appears maintain photosynthetic rates with minimal differences between plants grown under LL or HL conditions. Light response curves done with three different ambient CO₂ levels demonstrated that the Yukon ecotypes appears to acclimate to high irradiance using photorespiration as an energy sink and this hypothesis can explain why the plants of this ecotype grown under HL conditions does not exhibit the typical low- high- light

response when compared with plants grown under LL conditions. Tolerance to photoinhibition showed that the Yukon ecotype has a higher tolerance to photoinhibition than the Shandong ecotype under LL and HL conditions.

Future studies to unravel in detail the different photoacclimation mechanisms of these two ecotypes include assessing the contribution of PTOX in both ecotypes in response to HL growth irradiance and an analysis of key photorespiratory metabolites.

CHAPTER 6

6.0 References

- Adams WW, Watson AM, Mueh KE, Amiard V, Turgeon R, Ebbert V, Logan BA, Combs AF, Demmig-Adams B** (2007) Photosynthetic acclimation in the context of structural constraints to carbon export from leaves. *Photosynth Res* **94**:455-466
- Allen JF, Forsberg J** (2001) Molecular recognition in thylakoid structure and function. *Trends Plant Sci* **6**:317-326
- Amtmann A** (2009) Learning from evolution: *Thellungiella* generates new knowledge on essential and critical components of abiotic stress tolerance in plants. *Mol Plant* **2**:3-12
- Amtmann A, Bohnert HJ, Bressan RA** (2005) Abiotic stress and plant genome evolution. Search for new models. *Plant Physiol* **138**:127-130
- Anderson JM** (1986) Photoregulation of the composition, function, and structure of thylakoid membranes. *Annu Rev Plant Physiol* **37**:93-136
- Anderson JM, Chow WS, Park, YI** (1995) The grand design of photosynthesis: Acclimation of the photosynthetic apparatus to environmental cues. *Photosynth Res* **46**:129-139
- Anderson JM, Osmond CB** (1987) Shade-Sun Responses: Compromises Between Acclimation and Photoinhibition. In Kyle DJ, Osmond CB, Arntzen, CJ (eds.) *Topics in Photosynthesis*. Vol. 9. Photoinhibition. Elsevier, Amsterdam, pp 1-38
- Arnoux P, Morosinotto T, Saga G, Bassi R, Pignol D** (2009) A structural basis of the pH-dependent xanthophyll cycle in *Arabidopsis thaliana*. *Plant Cell* **21**:2036-2044
- Aro EM, Virgin I, Andersson B** (1993) Photoinhibition of photosystem II. Inactivation, protein damage and turnover. *Biochim Biophys Acta* **1143**:113-134
- Aro EM, Suorsa M, Rokka A, Allahverdiyeva Y, Paakkarinen V, Saleem A, Battchikova N, Rintamaki E** (2005) Dynamics of photosystem II: a proteomic approach to thylakoid protein complexes. *J Exp Bot* **56**:347-356
- Asada K** (1999) The water-water cycle in chloroplasts: scavenging of active oxygens and dissipation of excess photons. *Annu Rev Plant Physiol Plant Mol Biol* **50**:601-639
- Asada K** (2000) The water-water cycle as alternative photon and electron sinks. *Philos Trans R Soc Lond B Biol Sci* **355**:1419-1431
- Athanasidou K, Dyson BC, Webster RE, Johnson GN** (2010) Dynamic acclimation of photosynthesis increases plant fitness in changing environments. *Plant Physiol* **52**:366-373

Avenson TJ, Cruz JA, Kramer DM (2004). Modulation of energy-dependent quenching of excitons in antennae of higher plants. *Proc Natl Acad Sci USA* **101**:5530-5535

Backhausen JE, Scheibe R (1999) Adaptation of tobacco plants to elevated CO₂: influence of leaf age on changes in physiology, redox states and NADP-malate dehydrogenase activity. *J Exp Bot* **50**:665-675

Bailey S, Horton P, Walters RG (2004) Acclimation of *Arabidopsis thaliana* to the light environment: the relationship between photosynthetic function and chloroplast composition. *Planta* **218**:793-802

Bailey S, Walters RG, Jansson S, Horton P (2001) Acclimation of *Arabidopsis thaliana* to the light environment: the existence of separate low light and high light responses. *Planta* **213**:794-801

Baker NR (2008) Chlorophyll fluorescence: a probe of photosynthesis in vivo. *Annu Rev Plant Biol* **59**:89-113

Baker NR, Harbinson J, Kramer DM (2007) Determining the limitations and regulation of photosynthetic energy transduction in leaves. *Plant Cell Environ* **30**:1107-1125

Ballaré CL (1999) Keeping up with the neighbours: phytochrome sensing and other signalling mechanisms. *Trends Plant Sci* **4**:97-102

Bauwe H, Hagemann M, Kern R, Timm S (2012) Photorespiration has a dual origin and manifolds links to central metabolism. *Curr Opin Plant Biol* **15**:269-275

Beadle CL (1993) Growth Analysis. In Hall DO, Scurlock JMO, Bolhar-Nordenkapf HR, Leegood RC and Long SP, (eds.) *Photosynthesis and Production in a Changing Environment: A Field and Laboratory Manual*. Chapman & Hall, London, pp 36-46

Belgio E, Kapitanova E, Chmeliov J, Duffy CDP, Ungerer P, Valkunas L, Ruban AV (2014) Economic photoprotection in photosystem II that retains a complete light-harvesting system with slow energy traps. *Nat Commun* **5**:4433

Biswal B, Joshi PN, Raval MK, Biswal UC (2011) Photosynthesis, a global sensor of environmental stress in green plants: stress signalling and adaptation. *Curr Sci India* **101**:47-56

Block W, Lewis Smith RI, Kennedy AD (2009) Strategies of survival and resource exploitation in the Antarctic fellfield ecosystem. *Biol Rev Camb Philos Soc* **84**:449-84

Boardman NK (1977) Comparative photosynthesis of sun and shade plants. *Annu Rev Plant Physiol* **28**:355-377

Bowsher C, Steer M, Tobin A (2008) Plant Biochemistry. Garland Science, New York, 500 pp

Boyes DC, Zayed AM, Ascenzi R, McCaskill AJ, Hoffman NE, Davis KR, Gortach J (2001) Growth stage-based phenotypic analysis of *Arabidopsis*: a model for high throughput functional genomics in plants. *Plant Cell* **13**:1499-1510

Bressan RA, Zhang C, Zhang H, Hasegawa PM, Bohnert HJ, Zhu JK (2001) Learning from the *Arabidopsis* experience. The next gene search paradigm. *Plant Physiol* **127**:1354-1360

Brestic M, Cornic G, Fryer MJ, Baker NR (1995) Does photorespiration protect the photosynthetic apparatus in French bean leaves from photoinhibition during drought stress? *Planta* **196**:450-457

Caffarri S, Tibiletti T, Jennings RC, Santabarbara S (2014) A comparison between plant photosystem I and Photosystem II architecture and functioning. *Curr Protein Pept Sc* **15**:296-331

Carbonera D, Agostini G, Morosinotto T, Bassi R (2005) Quenching of chlorophyll triplet states by carotenoids in reconstituted *Lhca4* subunit of peripheral light-harvesting complex of photosystem I. *Biochemistry* **44**:8337-8346

Chalker-Scott L (1999) Environmental significance of anthocyanins in plant stress responses *Photochem Photobiol* **70**:1-9

Chapin FS III, Autimn K, Pugniare F (1993) Evolution of suits of traits in response to environmental stress. *Am Nat* **142**:78-92

Chow WS, Adamson HY, Anderson JM (1991) Photosynthetic acclimation of *Tradescantia albiflora* to growth irradiance: Lack of adjustment of light-harvesting components and its consequences. *Physiol Plant* **81**:175-182

Croce R, van Amerongen H (2013) Light-harvesting in photosystem I. *Photosynth Res* **116**:153-166

Cruz JA, Avenson TJ, Kanazawa A, Takizawa K, Edwards GE, Kramer DM (2005) Plasticity in light reactions of photosynthesis for energy production and photoprotection. *J Exp Bot* **56**:395-406

Demmig-Adams B, Adams WW III (1992) Photoprotection and other responses of plants to high light stress. *Annu Rev Plant Physiol Plant Mol Biol* **43**:599-626

Demmig-Adams B, Adams III WW (2000) Photosynthesis: harvesting sunlight safely. *Nature* **403**:371-374

Derks A, Schaven K, Bruce D (2015) Diverse mechanisms for photoprotection in photosynthesis. Dynamic regulation of photosystem II excitation in response to rapid environmental change. *Biochim Biophys Acta* **1847**:468-485

Des Marais DL, Juenger TE (2010) Pleiotrophy, plasticity, and the evolution of plant abiotic stress tolerance. *Ann NY Acad Sci* **1206**:56-79

Eberhard S, Finazzi G, Wollman FA (2008) The dynamics of photosynthesis. *Annu Rev Genet* **42**:463-515

Ensminger I, Busch F, Huner NPA (2006) Photostasis and cold acclimation: sensing low temperature through photosynthesis. *Physiol Plant* **126**:28-44

Evans JR (1987) The relationship between electron transport components and photosynthetic capacity in pea leaves grown at different irradiances. *Aust J Plant Physiol* **14**:157-170

Falkowski PG, Chen YB (2003) Photoacclimation of light harvesting systems in eukaryotic algae. In Green BR, Parson WW, (eds.) *Advances in Photosynthesis and Respiration. Light Harvesting Antennas in Photosynthesis*. Vol. 13. Kluwer Academic Publishers, Dordrecht, pp 423-447

Farquhar GD, von Caemmerer S, Berry JA (1980) A biochemical model of photosynthetic CO₂ assimilation in leaves of C₃ species. *Planta* **149**:78-90

Field C, Berry JA, Mooney HA (1982) A portable system for measuring carbon dioxide and water vapour exchange of leaves. *Plant Cell Environ* **5**:179-186

Frankze A, German D, Al-Shehbaz IA, Mummenhoff K (2009) *Arabidopsis* family ties: molecular phylogeny and age estimates in Brassicaceae. *Taxon* **58**:425-437

Gaspar T, Franck T, Bisbis B, Kevers C, Jouve L, Hausman JF, J Dommès (2002) Concepts in plant stress physiology: application to plant tissue cultures. *Plant Growth Regul* **37**:263-285

Gienapp P, Teplitsky J, Alho JS, Mills A, Merilä J (2007) Climate change and evolution: disentangling environmental and genetic responses. *Mol Ecol* **17**:167-179

Giordano M (2013) Homeostasis: An underestimated focal point of ecology and evolution. *Plant Sci* **211**:92-101

Givnish TJ (1988) Adaptation to sun and shade: A whole-plant perspective. *Aust J Plant Physiol* **15**:63-92

Gould KS (2004) Nature's Swiss army knife: The diverse protective roles of anthocyanins in leaves. *J Biomed Biotech* **5**:314-320

Gould KS, Markham KR, Smith RH, Goris JJ (2000) Functional role of anthocyanins in the leaves of *Quintinia serrata* A. Cunn. J Exp Bot **51**:1107-1115

Gray GR, Heath D (2005) A global reorganization of the metabolome in *Arabidopsis* during cold acclimation is revealed by metabolic fingerprinting. Physiol Plant **124**:236-248

Gray GR, Hope BJ, Qin XQ, Tayler BG, Whitehead CL (2003) The characterization of photoinhibition and recovery during cold acclimation in *Arabidopsis thaliana* using chlorophyll fluorescence imaging. Physiol Plant **119**:365-375

Griffith M, Timonin M, Wong ACE, Gray GR, Akhter SR, Saldanha M, Rogers MA, Weretilnyk EA, Moffatt BA (2007) *Thellungiella*: an *Arabidopsis*-related model plant adapted to cold temperatures. Plant Cell Environ **30**:529-538

Guevara DR, Champigny MJ, Tattersall A, Dedrick J, Wong CE, Li Y, Labbe A, Ping CL, Wang Y, Nuin P, Golding GB, Mccarry BE, Summers PS, Moffatt BA, Weretilnyk EA (2012) Transcriptomic and metabolomics analysis of Yukon *Thellungiella* plants grown in cabinets and their natural habitat show phenotypic plasticity. BMC Plant Biol **12**:175

Hagemann M, Fernie AR, Espie GS, Kern R, Eisenhut M, Reumann S, Bauwe H, Weber APM (2013) Evolution of the biochemistry of the photorespiratory C2 cycle. Plant Biology **15**:639-647

Harley PC, Sharkey TD (1991) An improved model of C3 photosynthesis at high CO₂: reversed O₂ sensitivity explained by lack of glycerate reentry into the chloroplast. Photosyn Res **27**:169-178

Harley PC, Thomas RB, Reynolds JF, Strain BR (1992) Modelling photosynthesis of cotton grown in elevated CO₂. Plant Cell Environ **15**:271-282

Hirth M, Dietzel L, Steiner S, Ludwig R, Weidenbach H, Pfalzand J, Pfannschmidt T (2013) Photosynthetic acclimation responses of maize seedlings grown under artificial laboratory light gradients mimicking natural canopy conditions. Front Plant Sci **4**:334

Hopkins WG, Hüner NPA (2003) Introduction to Plant Physiology. Wiley, New York, 560 pp

Horton P, Ruban A (2005) Molecular design of the photosystem II light harvesting antenna: photosynthesis and photoprotection. J Exp Bot **56**:365-373

Horton P, Wentworth M, Ruban A (2005) Control of the light harvesting function of chloroplast membranes: The LHCII-aggregation model for non-photochemical quenching. FEBS Lett **579**:4201-4206

Huang W, Zhang SB, Hu H (2014) Sun leaves up-regulate the photorespiratory pathway to maintain a high rate of CO₂ assimilation in tobacco. *Front Plant Sci* **5**:688

Hüner NPA, Bode R, Dahal K, Busch FA, Possmayer M, Szyszka B, Rosso D, Ensminger I, Krol M, Ivanov AG, Maxwell DP (2013) Shedding some light on cold acclimation, cold adaptation, and phenotypic plasticity. *Botany* **91**:127-136

Hüner NPA, Grodzinski B (2011) Photosynthesis and photoautotrophy. In Moo-Young M, (ed.) *Comprehensive Biotechnology*. Vol. 1 Elsevier, Amsterdam, pp 315-322

Hüner NPA, Öquist G, Hurry VM, Krol M, Falk S, Griffith M (1993). Photosynthesis, photoinhibition and low temperature acclimation in cold tolerant plants. *Photosyn Res* **37**:19-39

Hüner NPA, Öquist G, Sarhan F (1998) Energy balance and acclimation to light and cold. *Trends Plant Sci* **3**:224-230

Hüner NPA, Öquist G, Melis A (2003) Photostasis in plants, green algae and cyanobacteria: The role of light harvesting complexes. In Green BR, Parson WW, (eds.) *Light Harvesting Antennas in Photosynthesis*. Springer, Dordrecht, pp 404-421

Inan G, Zhang Q, Li P, Wang Z, Cao Z, Zhang H, Zhang C, Quist TM, Goodwin SM, Zhu J, Shi H, Damsz B, Charbaji T, Gong Q, Ma S, Fredricksen M, Galbraith DW, Jenks MA, Rhodes D, Hasegawa PM, Bohnert HJ, Joly RJ, Bressan RA, Zhu JK (2004) Salt cress: a halophyte and cryophyte *Arabidopsis* relative model system and its applicability to molecular genetic analyses of growth and development of extremophiles. *Plant Physiol* **135**:1718-1737

Ireland CR, Long SP, Baker NR (1989). An integrated portable apparatus for the simultaneous field measurements of photosynthetic CO₂ and water vapour exchange, light absorption and chlorophyll fluorescence emission of attached leaves. *Plant Cell Environ* **12**:947-958

Jenks M, Hasegawa P (2005) *Plant Abiotic Stress*. Blackwell Publishing, Oxford, 292 pp

Kant S, Bi YM, Weretilnyk E, Barak S, Rothstein SJ (2008) The *Arabidopsis* halophytic relative *Thellungiella halophila* tolerates nitrogen-limiting conditions by maintaining growth, nitrogen uptake, and assimilation. *Plant Physiol.* **147**: 1168-1180

Kasahara M, Kagawa T, Oikawa K, Suetsugu N, Miyao M, Wada M (2002) Chloroplast avoidance movement reduces photodamage in plants. *Nature* **420**:829-832

- Khanal N** (2011) Environmental Factors Influencing Growth, Freezing Tolerance and Photosynthesis in *Thellungiella* and *Arabidopsis*. PhD thesis, University of Saskatchewan, Canada
- Khanal N, Moffatt BA, Gray GR** (2015) Acquisition of freezing tolerance in *Arabidopsis* and two contrasting ecotypes of the extremophile *Eutrema salsugineum* (*Thellungiella salsuginea*) J Plant Physiol **180**:35-44
- Kimura M, Yamamoto YY, Seki M, Sakurai T, Sato M, Abe T, Yoshida S, Manabe K, Shinozaki K, Matsui M** (2003) Identification of Arabidopsis genes regulated by high light-stress using cDNA microarray. Photochem Photobiol **77**:226-233
- Koch MA, German DA** (2013) Taxonomy and systematics are key to biological information: *Arabidopsis*, *Eutrema* (*Thellungiella*), *Noccaea* and *Schrenkiella* (Brassicaceae) as examples. Front Plant Sci **4**:267
- Kozaki A, Takeba G** (1996) Photorespiration protects C3 plants from photooxidation. Nature **384**:557-560
- Krause GH, Weis E** (1991) Chlorophyll fluorescence and photosynthesis: the basics. Annu Rev Plant Physiol Plant Mol Biol **42**:313-349
- Krol M, Gray GR, Hüner NPA** (1995) Low-temperature stress and photoperiod affect an increased tolerance to photoinhibition in *Pinus banksiana* seedlings. Can J Bot **73**:1119-1127
- Lake JA, Woodward I, Quick WP** (2002) Long-distance CO₂ signalling in plants. J Exp Bot **53**:183-193
- Lambers H, Chapin III FS, Pons TL** (2008) Plant Physiological Ecology. Springer, New York, 610 pp
- Larkindake J, Vireling E** (2008) Core genome responses involved in acclimation to high temperature. Plant Physiol **146**:748-768
- Lawlor DW** (2001) Photosynthesis. Bios Springer, New York, 386 pp
- Lennon AM, Prommeenate P, Nixon PJ** (2003) Location, expression and orientation of the putative chlororespiratory enzymes, Ndh and IMMUTANS, in higher-plant plastids. Planta **218**:254-260.
- Leong TY, Anderson JM** (1984) Adaptation of the thylakoid membranes of pea chloroplasts to light intensities I. Study on the distribution of chlorophyll-protein complexes. Photosyn Res **5**:105-115

Li XP, Björkman O, Shih C, Grossman AR, Rosenquist M, Jansson S, Niyogi K (2000) A pigment-binding protein essential for regulation of photosynthetic light harvesting. *Nature* **403**:391-395

Li XP, Muller-Moule P, Gilmore AM, Niyogi K (2002) PsbS-dependent enhancement of feedback de-excitation protects photosystem II from photoinhibition. *Proc Natl Acad Sci USA* **99**:15222-7

Lichtenthaler HK, Wellburn AR (1983) Determination of total carotenoids and chlorophylls *a* and *b* of leaf extracts in different solvents. *Biochem Soc Trans* **11**:591-592

Long SP, Bernacchi CJ (2003) Gas exchange measurements, what can they tell us about the underlying limitations to photosynthesis? Procedures and sources of error. *J Exp Bot* **54**:2393–2401

Long SP, Farage PK, Garcia RL (1996) Measurement of leaf and canopy photosynthetic CO₂ exchange in the field. *J Exp Bot* **47**:1629-1642

Long SP, Hägren JE (1993) Measurement of CO₂ assimilation by plants in the field and laboratory. In Hall DO, Scurlock JMO, Bolhar-Nordenkampf HR, Leegood RC, Long SP, (eds.) *Photosynthesis and Productivity in a Changing Environment: A Field and Laboratory Manual*. Chapman and Hall, London, pp 129-167

Lunde C, Jensen PE, Rosgaard L, Haldrup A, Gilpin MJ, Scheller HV (2003) Plants impaired in state transitions can to a large degree compensate for their defect. *Plant Cell Physiol* **44**:44-54

Malik VM, Lobo JM, Stewart C, Irani S, Todd CD, Gray GR (2016) Growth irradiance affects ureide accumulation and tolerance to photoinhibition in *Eutrema salsigineum* (*Thellungiella salsuginea*). *Photosynthetica* **54**:93-100

Malkin R, and Niyogi K (2000). Photosynthesis. In Buchanan BB, Gruissem W, Jones RL, (eds.) *Biochemistry and Molecular Biology of Plants*. American Society of Plant Biologists, New York, pp 568-628

Maurino VG, Peterhansel C (2010) Photorespiration: current status and approaches for metabolic engineering. *Curr Opin Plant Biol* **13**:249-256

Maurino VG, Peterhansel C (2011) Photorespiration redesigned. *Plant Physiol* **155**:49-55

Melis A (1999) Photosystem-II damage and repair cycle in chloroplasts: what modulates the rate of photodamage *in vivo*? *Trends Plant Sci* **4**:130-135

- Minagawa J, Takahashi Y** (2004) Structure, function and assembly of Photosystem II and its light-harvesting proteins. *Photosynth Res* **82**:241-263
- Mithell P** (1966) Chemiosmotic coupling I oxidative and photosynthetic phosphorylation. *Biol Rev Biol P Camb* **41**:445-502
- Morita MT, Nakamura M** (2012) Dynamic behavior of plastids related to environmental response. *Curr Opin Plant Biol* **15**:722-728
- Mullineaux CW, Emlyn-Jones D** (2005) State transitions: an example of acclimation to low-light stress. *J Exp Bot* **56**:389-393
- Mulo P, Sirpio S, Suorsa M, Aro EM** (2008) Auxiliary proteins involved in the assembly and sustenance of photosystem II. *Photosynth Res* **98**:489-501
- Muraoka H, Tang Y, Terashima I, Koizumi H, Washitani I** (2000) Contributions of diffusional limitation, photoinhibition and photorespiration to midday depression of photosynthesis in *Arisaema heterophyllum* in natural high light. *Plant Cell Environ* **23**: 235-250
- Murchie EH, Asgar A, Herman T** (2015) Photoprotection as a trait for rice yield improvement: status and prospects. *Rice* **8**:31
- Murchie EH, Chen Y, Hubbart S, Peng SB, Horton P** (1999) Interactions between senescence and leaf orientation determine in situ patterns of photosynthesis and photoinhibition in field-grown rice. *Plant Physiol* **119**:553–564
- Murchie EH, Horton P** (1998) Contrasting patterns of photosynthetic acclimation to the light environment are dependent on the differential expression of the responses to altered irradiance and spectral quality. *Plant Cell Environ* **21**:139-148
- Murchie EH, Pinto M, Horton P** (2009) Agriculture and the new challenges for photosynthesis research. *New Phytol* **181**:532-52
- Neill SO, Gould KS** (2003) Anthocyanins in leaves: light attenuators or antioxidants? *Funct Plant Biol* **30**:865-873
- Niyogi K, Li XP, Rosenberg V, Jung HS** (2005) Is PsbS the site of non-photochemical quenching in photosynthesis? *J Exp Bot* **56**:375-382
- Ögren E** (1991) Prediction of photoinhibition of photosynthesis from measurements of fluorescence quenching components. *Planta* **184**:538-544
- Oguchi R, Hikosaka K, Hirose T** (2003) Does the change in light acclimation need leaf anatomy? *Plant Cell Environ* **26**:505-512

Olsson T, Leverenz JW (1994) Non-uniform stomatal closure and the apparent convexity of the photosynthetic photon flux density response curve. *Plant Cell Environ* **17**:701-710

Öquist G, Hüner NPA (2003) Photosynthesis of overwintering evergreen plants. *Annu Rev Plant Biol* **54**:329-355

Orsini F, D'Urzo MP, Inan G, Serra S, Oh DH, Mickelbart MV, Consiglio F, Li X, Jeong JC, Yun DJ, Bohnert HJ, Bressan RA, Maggio A (2010) A comparative study of salt tolerance parameters in 11 wild relatives of *Arabidopsis thaliana*. *J Exp Bot* **61**:3787-3798

Park YI, Chow WS, Anderson JM (1997) Antenna size dependency of photoinactivation of photosystem II in light-acclimated pea leaves. *Plant Physiol* **115**:151-157

Parsons R, Weyers JDB, Lawson T, Godber IM (1997) Rapid and straightforward estimates of photosynthetic characteristics using a portable gas exchange system. *Photosynthetica* **34**:265-279

Perchorowicz JT, Raynes DA, Jensen RG (1981) Light limitation of photosynthesis and activation of ribulose biphosphate carboxylase in wheat seedlings. *Proc Natl Acad Sci USA* **78**:2985-2989

Peltier G, Cournac L (2002) Chlororespiration. *Annu Rev Plant Biol* **53**:523-550

Prioul JL, Chartier P (1977) Partitioning of transfer and carboxylation components of intracellular resistance to photosynthetic CO₂ fixation: A critical analysis of the methods used. *Ann Bot* **41**:789-800

Ros R, Cascales-Minana B, Segura J, Anoman AD, Toujani W, Flores-Tornero N, Rosa-Tellez S, Munoz-Bertomeo J (2013) Serine biosynthesis by photorespiratory and non-photorespiratory pathways: an interesting interplay with unknown regulatory networks. *Plant Biol* **15**:707-712

Rosso D, Ivanov AG, Fu A, Geisler-Lee A, Hendrickson L, Geisler M, Stewart G, Krol M, Hurry V, Rodermeil SR, Maxwell DP, Hüner NPA (2006) IMMUTANTS does not act as a stress-induced safety valve in the protection of the photosynthetic apparatus of *Arabidopsis* during steady-state photosynthesis. *Plant Physiol* **142**:574-585

Ruban AV (2009) Plants in light. *Commun Integr Bio* **2**:50-55

Ruban AV, Johnson MP, Duffy CDP (2012) The photoprotective molecular switch in the photosystem II antenna. *Biochim Biophys Acta* **1817**:167-181

Scheibe R (2004). Malate valves to balance cellular energy supply. *Physiol Plant* **120**:21-26

Schlüter U, Muschak M, Berger D, Altmann T (2003) Photosynthetic performance of an *Arabidopsis* mutant with elevated stomatal density (*sdd1-1*) under different light regimes. *J Exp Bot* **54**:867-874

Sharkey TD, Bernacchi CJ, Farquhar GD, Singaas EL (2007) Fitting photosynthetic carbon dioxide response curves for C₃ leaves. *Plant Cell Environ* **30**:1035-1040

Sharkey TD, Berry JA, Raschke K (1985) Starch and sucrose synthesis in *Phaseolus vulgaris* as affected by light, CO₂, and abscisic acid. *Plant Physiol* **77**:617-620

Shirao M, Kuroki S, Kaneko K, Kinjo Y, Tsuyama M, Förster B, Takahashi S, Badger MR (2013) Gymnosperms have increased capacity for electron leakage to oxygen (Mehler and PTOX reactions) in photosynthesis compared with angiosperms. *Plant Cell Physiol* **54**:1152-63

Shötler MA, Tóth SZ (2014) Photosynthetic complex stoichiometry dynamics in higher plants: environmental acclimation and photosynthetic flux control. *Front Plant Sci* **5**:188

Somerville CR, Ogren WL (1982) Isolation of photorespiration mutants in *Arabidopsis*. In Edelman M, Hallick RB, Chua NH, (eds.) *Methods in Chloroplast Biology*. Elsevier, Amsterdam, pp 129-138

Stepien P, Johnson GN (2009) Contrasting responses of photosynthesis to salt stress in the glycophytic *Arabidopsis* and the halophytic *Thellungiella*: role of the plastid terminal oxidase as an alternative electron sink. *Plant Physiol* **149**:1154-1165

Streb P, Josse EM, Gallouet E, Baptist F, Kuntz M, Cornic G (2005) Evidence for alternative electron sinks to photosynthetic carbon assimilation in the high mountain plant species *Ranunculus glacialis*. *Plant Cell Environ* **28**:1123-1130

Stec B (2012) Structural mechanism of RuBisCO activation by carbamylation of the active site lysine. *Proc Natl Acad Sci USA* **109**:18785-18790

Stitt M (1986) Limitation of photosynthesis by carbon metabolism I. Evidence for excess electron transport capacity in leaves carrying out photosynthesis in saturating light and CO₂. *Plant Physiol* **81**:796-802

Sui N, Han G (2014) Salt-induced photoinhibition of PSII is alleviated in halophyte *Thellungiella halophila* by increases of unsaturated fatty acids in membrane lipids. *Acta Physiol Plant* **36**:983-992

Taiz L, Zeiger E (2006) *Plant Physiology*. Sinauer Associates, Sunderland, 700 pp

- Taji T, Seki M, Satou M, Sakurai T, Kobayashi M, Ishiyama K, Narusaka Y, Narusaka M, Zhu JK, Shinozaki K** (2004) Comparative genomics in salt tolerance between *Arabidopsis* and *Arabidopsis* –related halophyte salt cress using *Arabidopsis* microarray. *Plant Physiol* **135**:1697-1709
- Terashima I, Hanba YT, Tazoe Y, Vyas P, Yano S** (2006) Irradiance and phenotype: comparative ecocodevelopment of sun and shade leaves in relation to photosynthetic CO₂ diffusion. *J Exp Bot* **57**:343-354
- Tikkanen M, Grieco M, Nurmi M, Rantala M, Suorsa M, Aro EM** (2012) Regulation of the photosynthetic apparatus under fluctuating growth light. *Philos Trans R Soc Lond Biol Sci* **367**:3486-3493
- Timm S, Florian A, Arrivault S, Stitt M, Fernie AR** (2012) Glycine decarboxylase controls photosynthesis and plant growth. *FEBS Lett* **586**:3692-3697
- Timm S, Bauwe H** (2013) The variety of photorespiratory phenotypes – employing the current status for future research directions on photorespiration. *Plant Biol* **15**:737-747
- Vance CP, Uhde-Stone C, Allan DL** (2003) Phosphorus acquisition and use: critical adaptations by plants for securing a nonrenewable resource. *New Phytol* **157**:423-447
- Vishwakarma A, Bashyame L, Senthilkumaran S, Scheibe R, Padmasree K** (2014) Physiological role of AOX1a in photosynthesis and maintenance of cellular redox homeostasis under high light in *Arabidopsis thaliana*. *Plant Physiol Biochem* **81**:44-53
- von Caemmerer S, Farquhar GD** (1981) Some relationships between the biochemistry of photosynthesis and the gas exchange rates of leaves. *Planta* **153**:376-387
- Walters RG** (2005) Towards an understanding of photosynthetic acclimation. *J Exp Bot* **56**:435-447
- Walters RG, Horton P** (1994) Acclimation of *Arabidopsis thaliana* to the light environment: Changes in composition of the photosynthetic apparatus. *Planta* **195**:248-256
- Walters RG, Horton P** (1995) Acclimation of *Arabidopsis thaliana* to the light environment: Changes in photosynthetic function. *Planta* **197**:306-312
- Walters RG, Shephard F, Rogers JJ, Horton P** (1999) Acclimation of *Arabidopsis thaliana* to the light environment: the role of photoreceptors. *Planta* **209**:517-527
- Walters RG, Shephard F, Rogers JJ, Horton P** (2003) Identification of mutants of *Arabidopsis* defective in acclimation of photosynthesis to the light environment. *Plant Physiol* **131**:472-481

Wataru Y, Evnas JR, von Caemmerer S (2010) Effects of growth and measurement light intensities on temperature dependence of CO₂ assimilation rate in tobacco leaves. *Plant Cell Environ* **33**:332-343

Wingler A, Lea PJ, Quick WP, Leegood RC (2000) Photorespiration: metabolic pathways and their role in stress protection. *Philos Trans R Soc Lond B Biol Sci* **355**:1517-1529

Wilson KE, Ivanov AG, Öquist G, Grodzinski B, Sarhan F, Hüner NPA (2006) Energy balance, organellar redox status, and acclimation to environmental stress. *Can J Bot* **84**:1355-1370

Wong CE, Li Y, Whitty B, Akhter S, Diaz C, Brandle J, Golding B, Weretynylk E, Moffatt BA, Griffith M (2005) Expressed sequence tags from the Yukon ecotype of *Thellungiella salsuginea* reveal that gene expression in response to cold, drought and salinity shows little overlap. *Plant Mol Biol* **58**:561-574

Wong CE, Li Y, Labbe A, Guevara D, Nuin P, Whitty B, Diaz C, Golding GB, Gray GR, Weretynylk EA, Griffith M, Moffatt BA (2006) Transcriptional profiling implicates novel interactions between abiotic stress and hormonal responses in *Thellungiella*, a close relative of *Arabidopsis*. *Plant Physiol* **140**:1437-1450

Yamori W, Noguchi K, Hikosaka K, Terashima I (2010) Phenotypic plasticity in photosynthetic temperature acclimation among crop species with different cold tolerances. *Plant Physiol* **152**:388-399

Yang R, Jarvis DE, Chen H, Beilstein MA, Grimwood J, Jenkins J, Shu S, Prochnik S, Xin M, Ma C, Schmutz J, Wing RA, Mitchell-Olds T, Schumaker KS, Wang X (2013). The reference genome of the halophytic plant *Eutrema salsugineum*. *Front Plant Sci.* **4**:46

Yano S, Terashima I (2004) Developmental process of sun and shade leaves in *Chenopodium album* L. *Plant Cell Environ* **27**:781-793